Ryerson University
Digital Commons @ Ryerson

Theses and dissertations

1-1-2006

Novel power control and adaptive rate transmission in W-CDMA mobile systems

Gang Luo
Ryerson University

Follow this and additional works at: http://digitalcommons.ryerson.ca/dissertations

 Part of the Electrical and Computer Engineering Commons

Recommended Citation
Luo, Gang, "Novel power control and adaptive rate transmission in W-CDMA mobile systems" (2006). *Theses and dissertations.* Paper 428.

This Thesis is brought to you for free and open access by Digital Commons @ Ryerson. It has been accepted for inclusion in Theses and dissertations by an authorized administrator of Digital Commons @ Ryerson. For more information, please contact bcameron@ryerson.ca.

17114901

NOVEL POWER CONTROL AND ADAPTIVE RATE TRANSMISSION IN W-CDMA MOBILE SYSTEMS

by

Gang Luo
Bachelor of Science Degree in Electrical Engineering
Nanjing University of Post and Telecommunications, China, 1994

A thesis
presented to Ryerson University
in partial fulfillment of the
requirement for the degree of
Master of Applied Science
in the Program of
Electrical and Computer Engineering.

Toronto, Ontario, Canada, 2006

© Gang Luo, 2006

PROPERTY OF
RYERSON UNIVERSITY LIBRARY

UMI Number: EC53798

INFORMATION TO USERS

The quality of this reproduction is dependent upon the quality of the copy submitted. Broken or indistinct print, colored or poor quality illustrations and photographs, print bleed-through, substandard margins, and improper alignment can adversely affect reproduction.

In the unlikely event that the author did not send a complete manuscript and there are missing pages, these will be noted. Also, if unauthorized copyright material had to be removed, a note will indicate the deletion.

UMI®

UMI Microform EC53798
Copyright 2009 by ProQuest LLC
All rights reserved. This microform edition is protected against unauthorized copying under Title 17, United States Code.

ProQuest LLC
789 East Eisenhower Parkway
P.O. Box 1346
Ann Arbor, MI 48106-1346

Author's Declaration

I hereby declare that I am the sole author of this thesis.
I authorize Ryerson University to lend this thesis to other institutions or individuals for the purpose of scholarly research.

Gang Luo

I further authorize Ryerson University to reproduce this thesis by photocopying or by other means, in total or in part, at the request of other institutions or individuals for the purpose of scholarly research.

Gang Luo

Instructions on Borrowers

Ryerson University requires the signatures of all persons using or photocopying this thesis. Please sign below, and give address and date.

Name	Signature	Address	Date

Abstract

NOVEL POWER CONTROL AND ADAPTIVE RATE TRANSMISSION IN W-CDMA MOBILE SYSTEMS

©Gang Luo 2006

Master of Applied Science
Department of Electrical and Computer Engineering
Ryerson University

Radio resource management (RRM) plays an extremely important role in efficient utilization of the limited radio resources to provide guaranteed quality of service (QoS). Power and transmission rate control are considered as two primary RRM components in mobile cellular systems. The former method is well-known for upholding required signal quality and reducing the energy consumption, while the latter is used to maximize the system throughput.

In this thesis, the algorithm of simultaneously adapting transmission power and data rate to maximize system throughput and minimize the power consumption for W-CDMA systems is proposed [1]. The greedy rate packing (GRP) allocation scheme is applied in the rate adaptation, where the higher transmission rate is assigned to the users with better channel conditions meanwhile minimizing the transmission power. It can be interpreted that more resources, such as power and transmission rate, are allocated at time instants when channel conditions are favorable. As a result, the resource allocation will be working in an efficient way. Another problem in power control is that using fixed stepsize power control (FSPC) can not fully react to the changing of the fading fluctuations when mobile speed changes. A novel dynamic stepsize power control (DSPC) algorithm [2] is presented as well, so as to enhance the system performance.

The performance of the proposed algorithms are evaluated through computer simulations, and compared with the traditional approaches from the literature. We model and simulate all major components of the system within an accurate frame/time slot structure specified in the UMTS W-CDMA system. Numerical results verify that significant performance improvement can be achieved with the proposed algorithms.

Acknowledgment

This work has been supported by many people to whom I wish to express my gratitude.

I am extremely grateful to my thesis advisor, Dr. Lian Zhao, who was most responsible for helping me make this work a success. Her encouragement and guidance combined with a superior, in-depth knowledge of wireless technology have enabled me to complete this thesis. Dr. Zhao's patient and kindness have made her not only an excellent advisor, but also a friend.

I would like to acknowledge Dr. Alagan Anpalagan, Dr. Xavier Fernando and Dr. Truman Yang for agreeing to be my thesis committee and for reviewing my research work.

I wish to express my gratitude to all my friends who helped me over the past two years. My special thanks to my best friends Bob Coghill and Roy Yu who have given me tremendous support and generous help, since I moved to Canada.

My deep appreciation to my parents, my brother and sister-in-law and relatives, especially my aunt, uncle and cousin Zhihui Cai, for their love and support.

I thank God for all He has given to me. This has been a beautiful and unforgettable experience in my life. I hope that I will be capable of paying my share to humankind with all the knowledge I have learned and will continue to learn during my life.

Contents

List of Tables

List of Figures

Abbreviation List

1G/2G/3G	First/Secod/Third Generation
3GPP	3G Partnership Project
AWGN	Additive White Gaussian Noise
BER	Bit Error Rate
BPSK	Binary Phase Shift Key
BS	Base Station
CDMA	Code Division Multiple Access
CIR	Carrier-to-Interference Ratio
CN	Core Network
CSN	Circuit Switched Network
DS-CDMA	Direct Sequence -Code Division Multiple Access
DSPC	Dynamic Stepsize Power Control
E_b/I_o	Energy-to-Interference-Spectral-Density Ratio
EN	Eternal Network
ETSI	European Telecommunications Standards Institute
FDMA	Frequency-division Multiple Access
FER	Frame Error Rate
FSPC	Fixed Stepsize Power Control
GRP	Greedy Rate Packing
GSM	Global System for Mobile Communications
HSDPA	High-Speed Downlink Packet Data Access
ISDN	Internet Service Digital Network
MAI	multiple access interference
MRC	Maximal Ratio Combining
MS	Mobile Station
OFDM	Orthogonal Frequency Division Multiplex
OVSF	Orthogonal Variable Spreading Factor
PC	Power Control
PCC	Power Control Command
pdf	Probability Density Function
PG	Processing Gain

PSN	Packeted Switched Network
PSTN	Public Switched telephone Network
QAM	Quadrature Amplitude Modulation
QoS	Quality of Service
QPSK	Quadrature Phase Shift Key
RNC	Radio Network Controller
SF	Spreading Factor
SNR	Signal-to-Noise Ratio
SIR	Signal-to-Interference Ratio
TDMA	Time-division Multiple Access
TPC	Transmit Power Control
W-CDMA	Wideband Code Division Multiple Access
UE	User Equipment
UMTS	Universal Telecommunications Mobile System
UTRAN	UMTS Terrestrial Radio Access Network
VSG	Variable-Spreading Gain

Chapter 1

Introduction

Wireless cellular communication systems have experienced tremendous growth over the last decade, and this growth continues unabated worldwide. The first-generation (1G) systems were analog and provided wireless speech service. The major improvement in the transition to second-generation (2G) systems was the digital transmission technology, which enables the use of error correction coding and increases service quality and capacity. The 2G systems, like either the Global System for Mobile Communications (GSM) or narrow-band code Division Multiple Access (CDMA) system, have evolved further to provide the packet-switched data service in addition to the conventional circuit-switched services such as speech services.

The new infrastructures which are called third-generation (3G) systems are suitable for the transmission of high-speed wireless data, so as to provide multimedia communications, exploring the unlimited information of the Internet, watching TV channels, and many other services on small and handy mobile phones. Standardization of 3G mobile communication systems is now rapidly progressing in all major regions of the world. These systems that go under the European Telecommunications Standards Institute (ETSI) name of Universal Telecommunications Mobile System (UMTS) will extend the services provided by current 2G systems (GSM, IS-136, and IS-95) [3, 4]. To reach these novel services, the first step is to use a multiple access method that can support high data rate transmission over wireless and mobile channels. Wideband CDMA (W-CDMA) has been chosen to be the multiple access technique for 3G mobile communications [5, 6]. The reasons for this choice are discussed in

Section 1.2.

In a cellular system, the base stations (BS) represent the access points of the mobile stations (MS). The inherent limitations of the wireless networks include scarce radio spectrum, a highly erratic and essentially stochastic channel, and user mobility. One lesson of cellular telephone network operation is that effective radio resource management (RRM) is essential to promote the quality and efficiency of multi-user communication systems, see for example [7, 8, 9]. RRM regulates the sharing of the radio resources between users. In a W-CDMA network, there are two primary controllable radio resources: transmission power and data rate. Transmission power should be adjusted to the minimum power required to achieve the target Quality of Service (QoS). The system resource a user occupied can be related to the generated interference spectral density level, which is generally proportional to the received power level and therefore the date rate. Consequently, a large received power implies that the mobile user occupies a large portion of the system resources. The problem formulation for the classical fixed-rate power control is usually considered to find the minimum power assignment that supports the target carrier-to-interference ratio (CIR) for as many users as possible, see for example, [10, 11, 12, 13, 14]. Power control is not an easy task due to the time-varying fluctuation in the channel gain as well as the delay of the channel state information.

On the other hand, W-CDMA systems have intrinsic support for dynamic rate transmission, see for example, [15, 16, 17] and the references cited in. It means that users are allowed to transmit different data rates in the fixed-length time frames. Thus, combining the transmission power control and data rate control in an optimum way is an important approach for efficient RRM [18, 19, 20]. One of the important goals of the multiple access systems is to maximize the number of simultaneous users. If each mobile station is assigned the minimum resources just high enough for meeting its QoS requirement, the capacity of the system will be maximized. Another important goal for non-voice users is to maximize their data rates. All these issues will be discussed in Chapter 3.

Another problem in power control is that using fixed stepsize power control (FSPC)

algorithm can not fully react to the changing of the fading fluctuations when mobile speed changes. It needs a long tracking time when the difference between the target CIR^* and the received CIR is much large than the stepsize, and can not control the power of MS efficiently under the deep fade, see e.g. [21, 22, 23]. Hence, it is necessary to use variable stepsize to improve the system performance and throughput [24, 25, 26].

In this thesis, we focus on developing a combined power control and adaptive rate transmission algorithm. Since uplink (MS to BS) power control in CDMA cellular systems is the single most important requirement, in order to minimize the effects of relative multiple access interference (MAI), and hence, maximize the system capacity, only the uplink is considered in this work. The greedy rate packing (GRP) allocation scheme [27] is applied in the rate adaptation, where the higher transmission rate is assigned to the users with better channel conditions (higher channel gains) meanwhile minimizing the transmission power based on the power constraints. It can be interpreted that more resources, including power and transmission rate, are allocated at time instants when channel conditions are favorable. The link which is in deep fading will be assigned lower rate, or even be turned off when fading is lower than a predefined threshold. As a result, the resource allocation will be working in an efficient way. In addition, a novel dynamic stepsize power control (DSPC) algorithm is proposed in this work as well. The DSPC algorithm is based on the difference between the target CIR^* and the received CIR. During each power control cycle, the BS compares the received CIR with the target CIR^* to determine the current power control stepsize. If the region in which the received CIR falls is farther from the target CIR^*, a larger stepsize will be chosen to adjust the transmit power with a larger degree to well track the channel condition variation and to maintain the desired target value. Otherwise, a smaller stepsize will be used when the received CIR is closer to the target CIR^* to reduce the granular noise. Simulation results demonstrate the effectiveness of the proposed algorithms when compared with the traditional power control schemes. Although the topics are treated in a general way, more attention is given to the UMTS air interface.

1.1 Network Architecture of 3G Mobile Cellular Systems

A simplified network architecture of the UMTS is shown in Fig. 1.1 [5]. As seen in Fig. 1.1, the UMTS Terrestrial Radio Access Network (UTRAN) has two interfaces. The first interface is with User Equipment (UE) using WCDMA. While the second interface is with the Core Network (CN). The UTRAN consists of base stations and Radio Network Controllers(RNC). The core network is the interface between UTRAN and the External Network (EN). It contains two networks, the Circuit Switched Network (CSN), which is the same as the old GSM switching network and the Packet Switched Network (PSN), which is based on Internet Protocol (IP) address. The CSN is connected to the conventional switching systems, such as Public Switched Telephone Network (PSTN) and Internet Service Digital Network (ISDN). The PSN, on the other hand is connected to the Internet network.

Since the UTRAN proposal contains both frequency-division duplex (FDD) and time-division duplex (TDD) modes of operation, power control for both cases is employed. The general property of power control for the FDD mode is that power control consists of both fast uplink (from MS to BS) and fast downlink (from BS to MS) schemes. While the power control for TDD is slower than that for FDD mode [28]. It is well-known that the uplink power control is more important than downlink power control in a CDMA system. The uplink power control consists of a closed loop power control, an outer loop power control, and an open loop power control. The closed (fast) loop power control regulates the transmission power of all UE to minimize the interface between them. The control command is updated at a rate of 1500Hz. The outer (slow) power control updates the target CIR^*, which is determined by the Radio Network Controller (RNC). While open loop power control is used for the initial power setting. Detailed description of power control concept will be introduced in Chapter 3. Furthermore, the data rate can be updated and more details will be presented in Chapter 3.

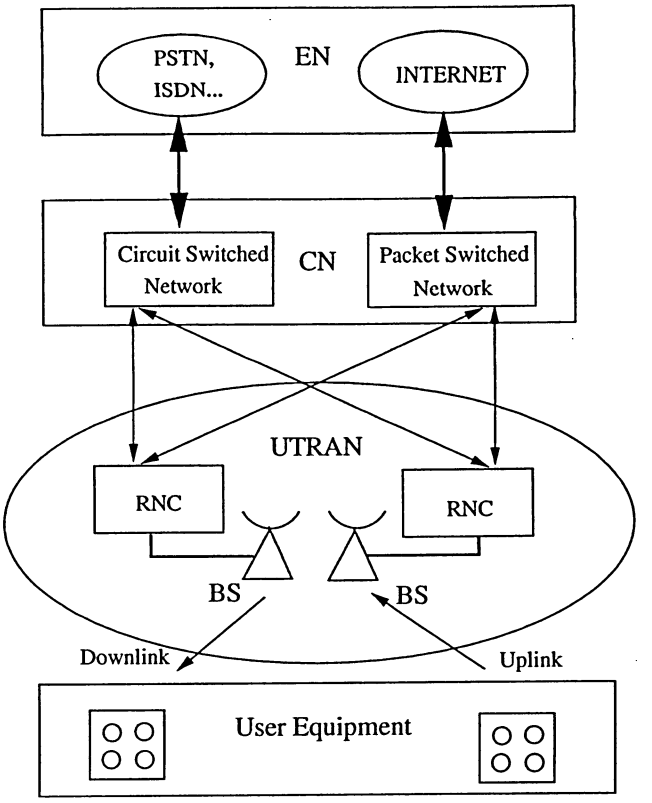

Figure 1.1: UMTS Network Architecture

1.2 Multiple Access Technology

In the multi-user environment, it is very important to separate the signals from different users, so that they are not interfering with each other. Multiple access is a signal transmission situation in which two or more users wish to simultaneously communicate each other by sharing the same propagation channel. In the uplink, particularly, multiple users will want to transmit information simultaneously. Without proper coordination among the transmitting users, collisions will occur when two or more users transmit at the same time. Multiple access strategies based on orthogonality among the competing transmissions are collision-free.

1.2.1 FDMA, TDMA and CDMA

Main techniques with built-in conflict resolution capability include frequency-division multiple access (FDMA), time-division multiple access (TDMA) and code-division multiple access (CDMA). Performance analysis and evaluation of these conflict-free multiple access methods are described and discussed, e.g., in [29, 30, 31].

In FDMA system, the total bandwidth of the system is divided into narrow frequency channels which are then allocated to the multiple users. The users of TDMA system are separated by assigning certain time slot for each user. While CDMA is a spread spectrum technology, where each user is assigned a pseudo-random spreading code. Thus, all users simultaneously share the same bandwidth, but with different codes, as illustrated in Fig. 1.2.

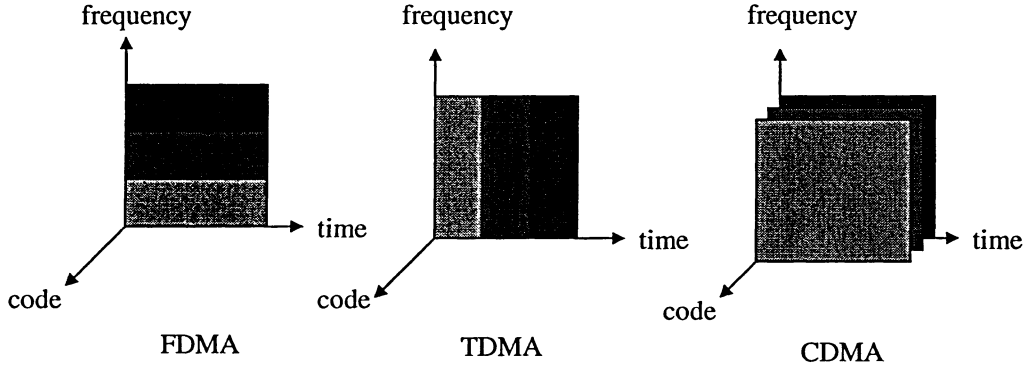

Figure 1.2: Multiple Access Schemes: FDMA, TDMA, and CDMA

CDMA has many advantages over TDMA or FDMA technologies. First of all, CDMA techniques are wideband in the sense that the entire transmission bandwidth is shared among all the users at all times. This is accomplished by spreading the baseband signals onto a bandwidth which is much larger than its original bandwidth. As a result, CDMA offers more bandwidth efficiency than plain FDMA or TDMA. Another benefit of employing CDMA is the use of the *RAKE* receiver, which can constructively combine multipath components, thus mitigating channel fading that afflicts narrowband systems. Furthermore, the use of voice

activity (reducing the transmission rate during silent period in a conversation) decreases interference and thus enhances the system throughput. It is then possible in the CDMA environment to provide unique benefits for cellular applications [32]. CDMA systems are interference limited and suffer from a phenomenon known as the *near-far* effect where the stronger received signal level raises the noise floor at the base station for the weaker signals. Power control is used in CDMA system implementation to combat this problem. Some of main features of CDMA are listed as follows:

- Several users use the same frequency with TDD or FDD mode.
- Unlike FDMA and TDMA, the CDMA system has soft capacity limits.
- Multipath fading is reduced due to the spreading of the message signal.
- The channel data rate of CDMA system may be high due to the fact that the bandwidth is higher than that of the FDMA or TDMA system.
- The near-far problem limits the performance of the system, if power control scheme is not correctly applied.
- Multi-access interference limits the performance of the CDMA system.

The second-generation CDMA cellular system is considered as a narrowband CDMA system [33]. In the narrowband CDMA system the available wideband spectrum is divided into a number of small bandwidth spectrums. Each of these sub-channels forms a narrowband CDMA system where the processing gain (PG) is lower than that for the original wideband CDMA system. Fig. 1.3 illustrates the spectrum of the narrowband and the wideband CDMA system. This type of system is called TDMA/CDMA or FCDMA system. The advantage of the FCDMA system is that different users can be allocated different bandwidth depending on their requirement.

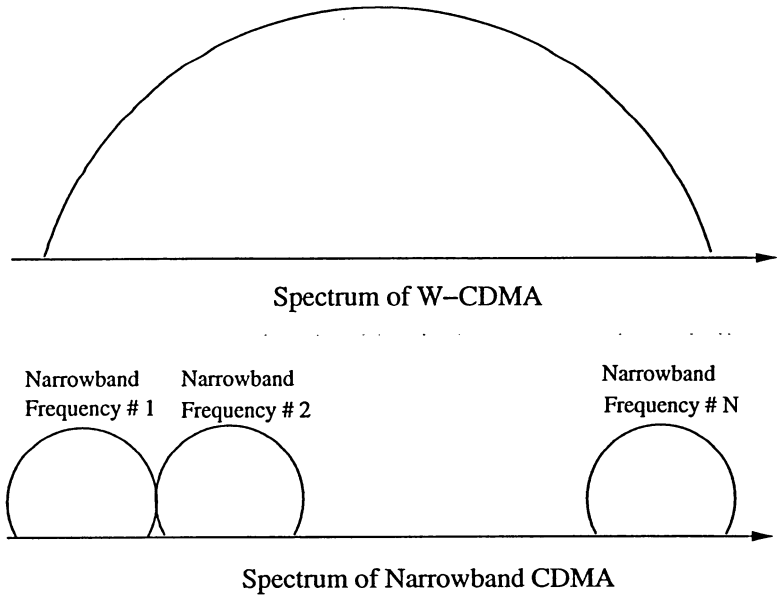

Figure 1.3: Specrum of W-CDMA Compared to the Narrowband CDMA

1.2.2 Wideband CDMA System

In W-CDMA systems, the transmission bandwidth of a signal channel is much larger than the coherence bandwidth of the channel. It offers significant improvements such as increased coverage and capacity due to a higher bandwidth compared to the 2G narrow-band CDMA system. Table 1.1, illustrates the key parameters of the W-CDMA system [5].

Multiple access scheme	Wideband DS-CDMA
Duplex scheme	FDD/TDD
Chip rate	4.096 Mcps (8.192/16.384 Mcps)
Carrier spacing	4.4-5.0 MHz
Modulation scheme	Quadrature Phase Shift Key (QPSK)
Channel coding	Convolutional and turbo codes
Multirate	Variable spreading and multicode
Spreading factors	4-256 (uplink), 4-512 (downlink)

Table 1.1: Key Parameters of W-CDMA system

- *W-CDMA physical channel structure*:

W-CDMA defines two types of dedicated physical channels. One is the Dedicated Physical Data Channel (DPDCH) which is used to carry dedicated data generated at layer 2 and above. The other one is the Dedicated Physical Control Channel (DPCCH) which is used to carry layer 1 control information. In the uplink, the DPDCH and DPCCH are coded. The In-phased and Quadrature bits are multiplexed within each radio frame. The uplink DPDCH carries the control data while the DPCCH carries pilot bits, and Transmit Power Control (TPC) commands [5]. In the basic operation, each physical channel is organized in a frame structure. Each frame of length 10 ms is divided into 15 time slots of length 0.625 ms so that each slot consists 2560 chips each corresponding to one power control period. Therefore, the power control and pilot symbol frequency is 1500 Hz. For the downlink (BS to MS), pilot symbols are time-multiplexed with data symbols. Every slot starts with a group of pilot symbols (4 or 8) that may be used to estimate or predict the channel and perform synchronization. The frame/time slot structure for the uplink is shown in Fig. 1.4 where the transmitted data and control information such as TPC (transmit power control command) and TFCI (transport format combination indicator) are code multiplexed.

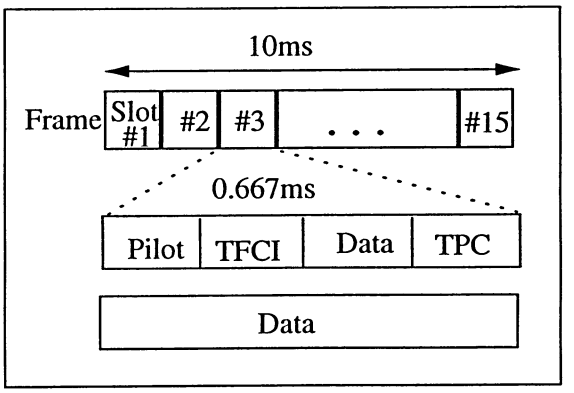

Figure 1.4: Uplink DPCCH/DPDCH Frame Structure of UMTS W-CDMA with $10ms$ Frame Length

- *Orthogonal variable-length code*:

Improving the capacity of multimedia communications is one of the targets for W-CDMA mobile communication systems. W-CDMA is designed to support a variety of data services

from voice to high-speed data and video. All users in the system have the same signal bandwidth and spread to the same chip rate. Thus, multi-rate transmission requires programmable Spreading Factor (SF).

Let each bit of the lowest bit-rate service be R_{min} and let it be spread by a code of length $M = 2^m$, when $m = 1, 2, \cdots, \log_2 R_{max}/2$. Also, let us assume that another low bit-rate service is transmitting at $2 \cdot R_{min}$ where the bit duration is half that for the previous case. Then, we need a spreading code of length $M/2 = 2^{n-1}$ for spreading. In general a code length of 2^{n-k} is needed for bit rate $2^k R_{min}$. A method to obtain variable-length orthogonal codes that preserve orthogonality between users at different transmission bit-rates is presented in [34].

The orthogonal variable spreading factor (OVSF) code or the signature sequence is used to spread the data to the chip rate. The OVSF codes can be defined in a tree-like manner illustrated in Fig. 1.5.

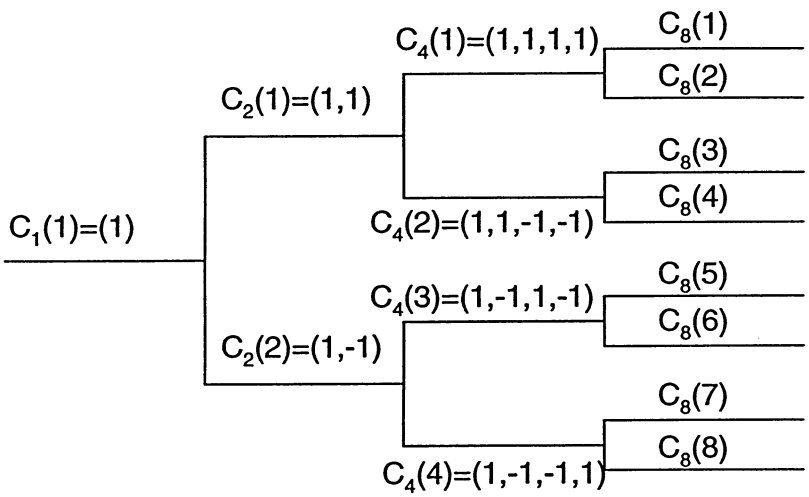

Figure 1.5: OVSF Code Tree

Starting from $C_1(1) = 1$, a set of 2^k spreading codes with the length of 2^k chips are generated at the kth layer. Generated codes of the same layer constitute a set of Walsh functions and they are orthogonal. In other words, a code can be selected in a system if and only if no other code on the path from the specific code to the root of the tree or the

sub-tree is selected in the same BS [35].

From this observation, we can easily find that if $C_8(1)$ is assigned to a user, all $\{C_{16}(1)$, $C_{16}(2)$, $C_{32}(1)$, $\cdots$, $C_{32}(4)$, $C_{64}(1)$, $\cdots$, $C_{64}(8)$, $C_{128}(1)$, $\cdots\}$ generated from the code cannot be assigned to other users requesting lower rates. The same provision applies for the mother codes that cannot be assigned to other users requesting higher rates. Therefore, the total number of codes is not fixed. However, it depends on the rate and spreading factor of each physical channel. Smaller spreading factors are selected for higher transmission rates while larger spreading factors are used for the lower transmission rate.

1.3 Cellular Radio System

The concept of cellular radio, which dates back to the 1960s [30], allows channels to be reused over the geographical area having sufficient spatial separation. To cover a large area with mobile communication services, the areas are divided into small subareas, called cells, each of which is served by a base station. The sizes of the cells can vary depending on the type of the area that they serve. For example, in a rural area with low density of users, the cells can be quite large (say, several kilometers in radius). These cells are referred to as *macro cells*. The cell sizes diminish when the number of potential users grows, like in cities and their central parts, where the cell radiuses can range from a few hundred meters to tens of meters (*micro cells*) or even meters (*pico cells*) covering, for example, a signal room in a building.

If omnidirectional antennas are used in the base station, the cell shape is ideally a circle. In practice, however, a cell takes a rather irregular shape due to the random effects. Moreover, for modelling and planning purpose, the circular form is not the most convenient one, since a plane filled up with circles can exhibit overlapped areas or gaps. Therefore, the shape of a cell is typically modelled as a regular polygon, such as an equilateral triangle, square, or hexagon, the hexagon being the most widely used shape. Of these shapes, the hexagonal array requires fewer cells for a given coverage area than a triangular and square array [32].

The beauty of the use of the cells instead of a signal base station is that the transmission

power of the cells can be kept small, and, most importantly, the transmission frequency of a particular cell can be reused in another cell, which increases the capacity of the system tremendously. The cells using the same frequency must be located sufficiently apart so that the *co-channel interference* is kept in tolerable limits. Fig. 1.6 shows an example of a hexagonal cellular layout with reuse factor 7. It can be seen that each cell has its own base station and users are randomly located in the system. The uniformly dispersed mobile users are displayed by small squares in the figure.

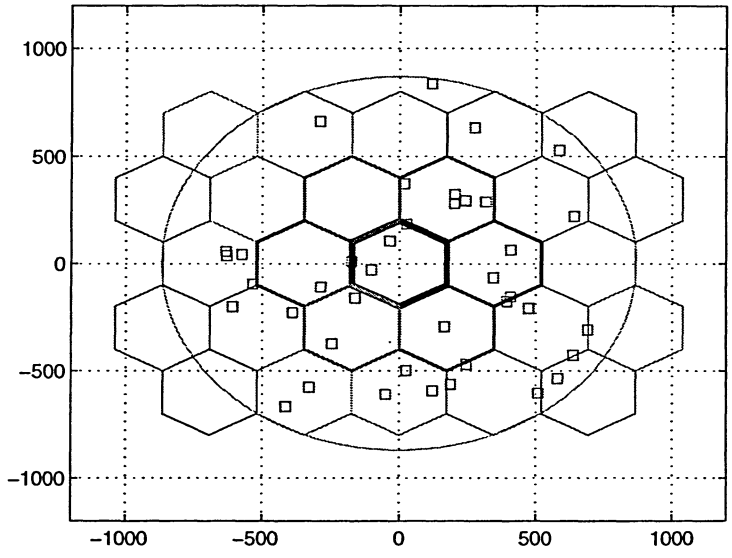

Figure 1.6: The Structure of Cellular Radio System

It is also possible to use directional instead of omnidirectional antennas at the base stations. Typically, the base station is equipped with three directional antennas, each covering a 120° sector. This can further increase network capacity, and decrease the cost of the system, since the base station equipment is utilized more efficiently.

1.4 Thesis Contributions

In this thesis, we focus on the power control and transmission rate adaptation techniques employed in the UMTS W-CDMA system. This research work has some general contributions that can be summarized as follows:

- **Combined power control and transmission rate adaptation algorithm**[1]:

Rate adaptation is first formulated as a maximum throughput problem. In the formulation, dynamical behavior of the mobile communication channel is also taken into consideration. A land mobile radio channel for urban areas is used for the channel model. In addition, a mathematical model of multipath fading is also defined to study and discuss the fading effects of wireless channels. More details can be found in Chapter 2. We apply the greedy rate packing (GRP) algorithm [27] to allocate the data rate, and correspondingly, the target CIR^*, of the users with the aid of their channel state information. A set of predefined target $CIRs^*$ are assigned to the users. The users' transmission rate is based on the channel condition. As a result, the rate assignment and target CIR^* assignment are interchangeable. Next, power control procedure starts in terms of the assigned target CIR^* and received CIR of every user. Furthermore, We apply our proposed algorithms to a frame/time slot structure of UMTS W-CDMA systems. Consequently, the transmission power is updated slot by slot, while the data rate is updated frame by frame. Simulation studies show the superiority of the proposed algorithm over several other algorithms from the literature. This topic is presented in Chapter 3, Section 3.3.

- **Dynamic stepsize power control algorithm**[2]:

A novel variable stepsize power control algorithm is proposed to enhance the system performance. The dynamic stepsize is based on the difference between the target CIR^* and the received CIR. The proposed DSPC algorithm is also applied in a frame/time slot structure and examined by analytical methods and extensive computer simulations. The system performance including throughput, BER, average transmission power consumption

etc., is evaluated. Besides, the $2ms$ frame length is also applied in the simulations. Moreover, some key parameters of the both FSPC and DSPC algorithms, such as *loop delay* (D), *PCC channel errors*, are analyzed and examined as well. The details of our proposed DSPC algorithm are covered in Chapter 4.

1.5 Thesis Outline

This thesis discusses two major topics in W-CDMA systems, namely power control and adaptive data transmission techniques.

The remaining of the thesis is organized as follows: Chapter 2 presents wireless channel characteristics. The mathematical model for multipath fading is studied and some main channel models are illustrated. Power control and rate adaptation in CDMA cellular communication systems are extensively discussed in Chapter 3, which gives the necessary background to understand the contributions made in the thesis. A literature survey of these topics is provided as well. Our proposed combined power control and transmission rate adaptation algorithm is also demonstrated. Furthermore, the numerical results and discussions will show the effectiveness of the proposed algorithm. In Chapter 4, a novel dynamic stepsize power control (DSPC) algorithm is introduced for the W-CDMA systems. It is shown that DSPC algorithm outperforms the conventional fixed stepsize power control (FSPC) approach. Finally, our conclusions and remarks are given in Chapter 5.

Chapter 2

Channel Characteristics of Mobile Radio Systems

2.1 Properties of Mobile Radio Channels

Radio waves propagate from a transmitting antenna, and travel through free space undergoing absorption, reflection, refraction, and scattering. The behavior of a typical mobile wireless channel is considerably more complex than that of an additive white Gaussian noise (AWGN) channel. Besides the thermal noise at the receiver front end (which is modeled by AWGN), the transmitted signals often experience channel fading and time dispersion due to user mobility and multipath propagation. Channel fading can be divided into large-scale fading and small-scale fading. Fig. 2.1 shows an overview of fading channel manifestations [36]. Large-scale fading, characterized by path loss and shadowing, represents the average signal power attenuation or path loss because of the motion over large area. While the small-scale fading is a characteristics of radio propagation resulting from the presence reflectors and scatterers that cause multiple versions of the transmitted signal to arrive at the receiver, each distorted in amplitude, phase and angle of arrival [30].

- **Path Loss**: It describes the loss in power as the radio signal propagates in space.
- **Shadowing**: It occurs due to the presence of fixed obstacles in the propagation path of the radio signal.

- **Multipath Fading**: It accounts for the combined effect of multiple propagation paths, rapid movements of mobile units (transmitters/receivers) and reflectors.

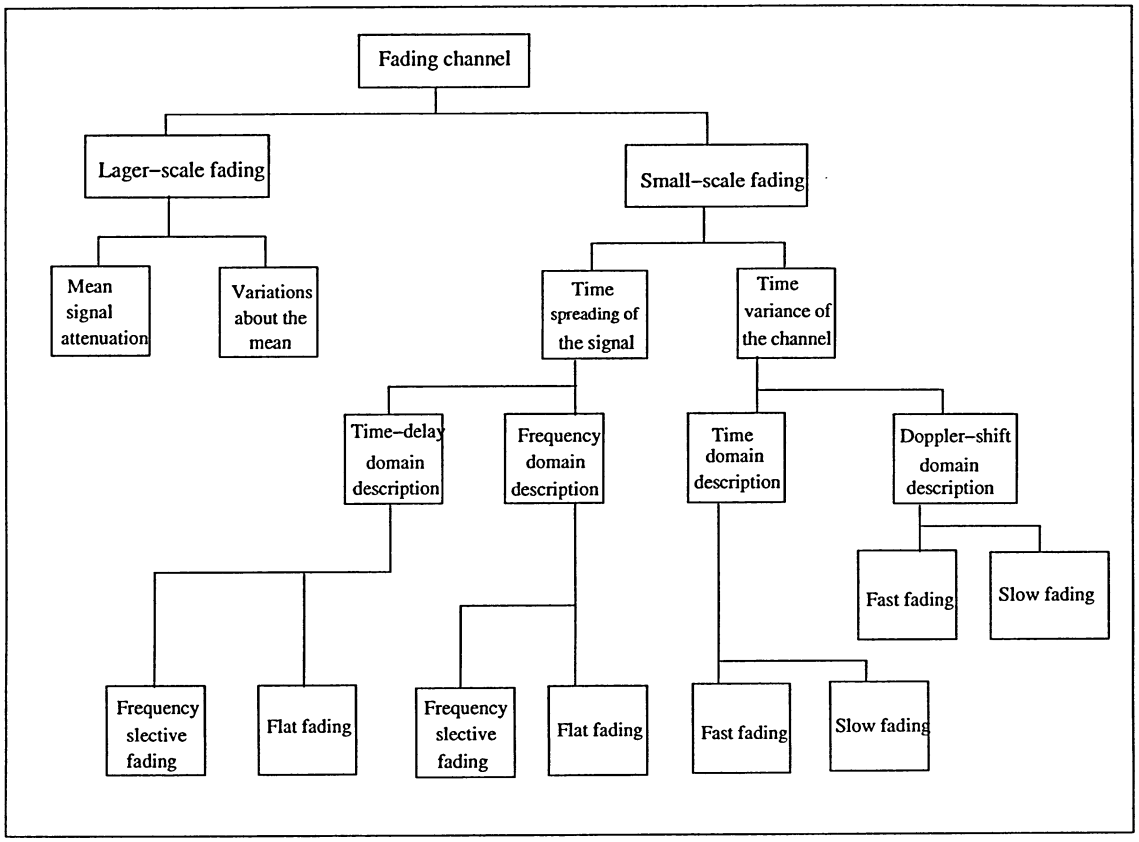

Figure 2.1: Overview of Channel Fading

2.1.1 Path Loss

In wireless channel, signals attenuate as they propagate. For a radio wave transmitted by a point source in free space, the loss in power, know as *path loss*, is given by

$$L = \left(\frac{4\pi d}{\lambda}\right)^2 \tag{2.1}$$

where λ is the wavelength of the signal, and d is the distance between the source and the receiver. The power of the signal decays as the square of the distance. In land mobile wireless

communication environments, similar situations are observed. The mean power of a signal decays as the nth power of the distance:

$$L = cd^n \tag{2.2}$$

where c is a constant and the exponent n typically ranges from 2 to 5 [37]. The exact values of c and n depend on the particular environment. The loss in power is a factor that limits the coverage of a transmitter.

2.1.2 Shadowing

Shadowing is due to the presence of large-scale obstacles in the propagation path of the radio signal. Due to the relatively large obstacles, movements of the mobile stations do not affect the short-term characteristics of the shadowing effect. Instead, the natures of the terrain surrounding the base station and the mobile stations as well as antenna heights determine the shadowing behavior.

Usually, shadowing is modeled as a slow time-varying multiplicative random process. Neglecting all other channel impairments, the received signal $r(t)$ is given by

$$r(t) = g(t)s(t) \tag{2.3}$$

where $s(t)$ is the transmitted signal and $g(t)$ is the random process which models the shadowing effect. For a given observation interval, we assume that $g(t)$ is a constant g, which is usually modeled as a log-normal random variable [37], G, whose density function is given by

$$f_G(g) = \begin{cases} \frac{1}{\sqrt{2\pi}\cdot\sigma\cdot g} \exp\left(-\frac{(\ln g-\mu)^2}{2\sigma^2}\right) & g \geq 0 \\ 0 & g < 0 \end{cases} \tag{2.4}$$

We notice that $\ln g$ is a Gaussian random variable with mean μ and variance σ^2. This translates to the physical interpretation that μ and σ^2 are the mean and variance of the loss measured in decibels (up to a scaling constant) due to shadowing. For cellular and micro cellular environment, the dB spread, σ, which is a function of the terrain and antenna heights, can range from 4 to 12dB [37].

2.1.3 Multipath Fading

In most of the mobile or cellular systems, the height of the mobile antenna may be smaller than the surrounding structures. Thus, the existence of a direct or *line-of-sight* path between the transmitter and the receiver is highly unlikely. In such a case, propagation is mainly due to reflection and scattering from the buildings and by diffraction over and/or around them. As a result, in practice, the transmitted signal arrives at the receiver via several different time delays creating a *multipath* situation.

Fading is the term used to describe the rapid fluctuations in the amplitude of the received radio signal over a short period of time. It is a common phenomenon in mobile communication channels caused by the interference between two or more versions of the transmitted signals which arrive at the receiver at slightly different times. The resultant received signal can vary widely in amplitude and phase, depending on various factors such as the intensity, relative propagation time of the waves, bandwidth of the transmitted signal, *etc.*

There are different types of fading according to the relation between signal and channel parameters. Based on multipath time delay (time domain), signal fading can be either flat or frequency selective determined comparing the signal bandwidth to the coherence bandwidth of the channel which can be defined as the maximum frequency separation for which the signals are still correlated. If the coherence bandwidth is greater than the signal bandwidth, the transmitted signal undergoes *flat fading.* Otherwise, the transmitted signal undergoes *frequency-selective fading.* On the other hand, based on Doppler spread (frequency domain), signal fading can be either fast or slow. Relative motion between the transmitter and the receiver results in Doppler spread in the received signal. If the Doppler spread of the channel is much less than the signal bandwidth, the signal undergoes *slow fading.* Practically, *fast fading* occurs at low data rates. Fig. 2.2 illustrates the classification of small-scale fading. It is noted that the coherence time which gives a measure of time duration over which the channel impulse response is essentially invariant (or highly correlated) should be less than the loop back delay of power control implemented in CDMA systems.

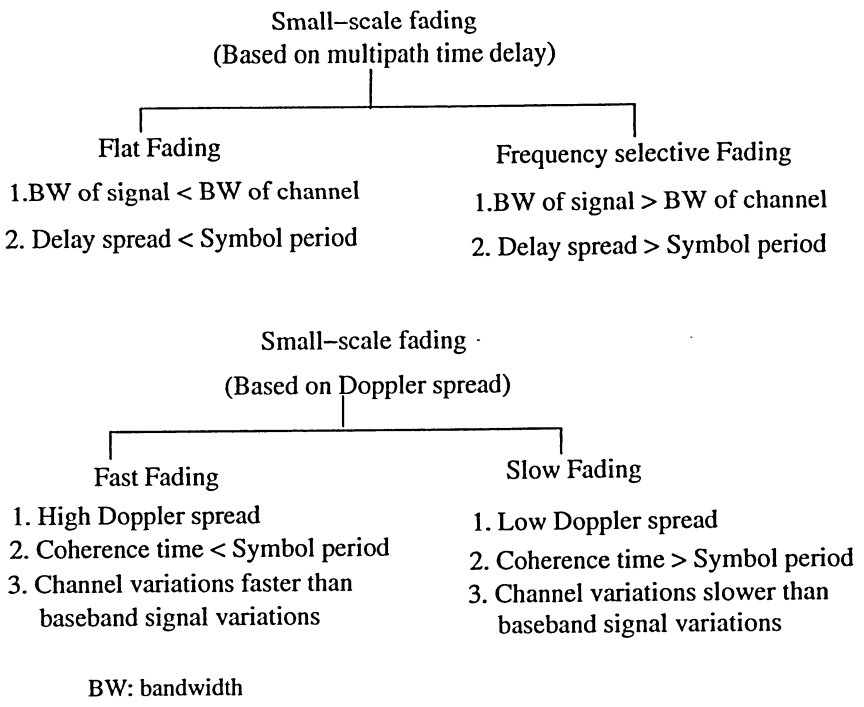

Figure 2.2: Classification of Small-Scale Fading

2.2 Statistical Fading Models

2.2.1 The Mathematical Model for Fading Channels

In Clarke-Jakes fading model [38], consider a transmitted signal at the tth time instant, $s(t)$ $= A\cos 2\pi f_c t$ through a multipath fading channel. Ignoring the effects of noise, the received signal which consists of a large number of multipath components that arrive uniformly from all angles can be expressed as:

$$r(t) = A\sum_{i=1}^{L} a_i \cos(2\pi f_c t + \theta_i) \tag{2.5}$$

where the variables a_i and θ_i are the attenuation and the phase-shift of the ith multipath component, respectively. The factor A denotes the signal amplitude. The above expression can be rewritten as:

$$r(t) = A\left\{\left(\sum_{i=1}^{L} a_i \cos(\theta_i)\right)\cos(2\pi f_c t) - \left(\sum_{i=1}^{L} a_i \sin(\theta_i)\right)\sin(2\pi f_c t)\right\} \tag{2.6}$$

Let

$$X_1(t) = \sum_{i=1}^{L} a_i \cos(\theta_i) \qquad X_2(t) = \sum_{i=1}^{L} a_i \sin(\theta_i).$$

The above equation becomes:

$$r(t) = A\left(X_1(t)\cos(2\pi f_c t) - X_2(t)\sin(2\pi f_c t)\right) \tag{2.7}$$

When there are a large number of scatters in the channel that contribute to the signal at the receiver, $X_1(t)$ and $X_2(t)$ become Gaussian variables with zero mean and σ^2 variance according to the central limit theorem [31]. Eq. (2.7) can be written as:

$$r(t) = AR(t)cos(2\pi f_c t + \theta(t)) \tag{2.8}$$

where the amplitude $R(t)$ and the phase $\theta(t)$ of the received waveform $r(t)$ are given respectively by:

$$R(t) = \sqrt{X_1(t)^2 + X_2(t)^2} \tag{2.9}$$

$$\theta(t) = \tan^{-1}\left(\frac{X_2(t)}{X_1(t)}\right), \tag{2.10}$$

Since the process $X_1(t)$ and $X_2(t)$ are Gaussian with zero mean, the envelope of the channel response at any time instant, $R(t)$, has a Rayleigh distribution and the phase is uniformly distributed in the interval $[0, 2\pi]$ with a probability density function (pdf) given by:

$$f_\theta(\theta) = \frac{1}{2\pi} \quad (0 \leq \theta \leq 2\pi) \tag{2.11}$$

The distortion in the phase can be easily overcome if differential modulation is employed. Whereas an amplitude distortion $R(t)$ severely degrades the performance of digital communication systems over fading channels. It is usually reasonable to assume that the fading stays essentially constant for at least one signaling interval.

2.2.2 Rayleigh Fading Model

Fading signal amplitude in large cells (macro-cellular environment) in the absence of a direct line of sight (Non-LOS) component is usually modeled as a Rayleigh random variable. It is well known that the random variable obtained by finding the square-root of the sum of the squares of two independent Gaussian random variables has a Rayleigh Distribution. The Rayleigh pdf is given as:

$$f_R(r) = \frac{r}{\sigma^2} \exp\left(\frac{-r^2}{2\sigma^2}\right) \quad (r \geq 0) \tag{2.12}$$

and

$$\sigma^2 = \frac{E[r^2]}{2} \tag{2.13}$$

where $E[\cdot]$ represents the expectation operation. Also note that Rayleigh fading is a good model for cellular mobile radio. Fig. 2.3 shows the simulated Rayleigh fading envelope using Clark-Jakes model with mobile speed at 50km/h, carrier frequency at 2GHz and sample frequency at $5kHz$, and the number of multipath component $L = 1$ and $L = 2$ using maximal ratio combining (MRC) at the receiver, respectively.

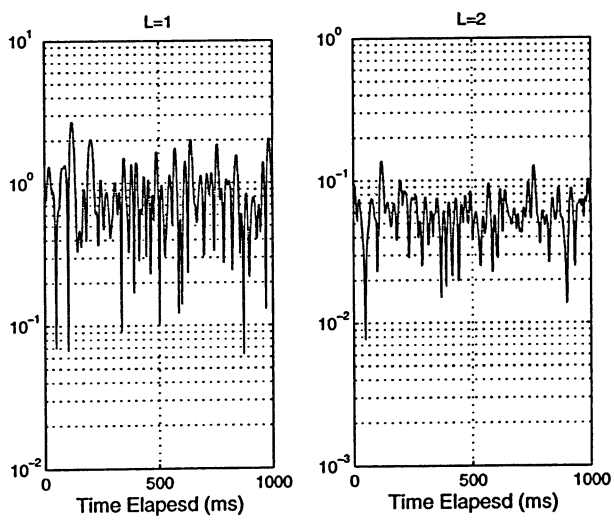

Figure 2.3: Simulated Rayleigh Fading Signal with Single and Two Path Envelope

When there are fixed scatterers or signal reflections in the medium in addition to randomly moving scatterers, $R(t)$ can no longer be modeled as having zero mean. In this case,

the envelop $R(t)$ has a Rician distribution and the channel is said to be a Rician fading channel.

2.2.3 Rician Fading Model

The Rician distribution is observed when, in addition to the multipath components, there exists a line of sight (LOS) path between the transmitter and the receiver. Indoor fading is often expected to be Rician distributed. This is common in micro-cellular systems. The probability density function for the envelop of the received signal is then given by:

$$f_R(r) = \frac{r}{\sigma^2} \exp\left(-\frac{r^2 + A^2}{2\sigma^2}\right) I_0\left(\frac{A \cdot r}{\sigma^2}\right) \qquad (r \geq 0, A > 0) \tag{2.14}$$

where factor A denotes the peak amplitude of the dominant signal and $I_0(\cdot)$ is the modified Bessel function of zero order. The Rician distribution is often described in terms of a parameter K, called Rician factor, which is defined as the ratio between the deterministic signal power and the variance of the multipath, given by $K = \frac{A^2}{2\sigma^2}$ or, in terms of dB: $K(dB) = 10\log(A^2/2\sigma^2)(dB)$. As A tends to zero and the dominant path decreases in amplitude, Rician distribution degenerates to a Rayleigh distribution. Fig. 2.4 presents the pdf of Rician distribution with a function of r and Rician factor K.

2.2.4 Nakagami-m Fading Model

The Nakagami-m distribution with fading severity index m, $m \geq 1/2$, is a versatile statistical model. It models signals that experience either less or more severe fading than that of Rayleigh distribution and sometimes fits experimental data much better than Rayleigh or Rician distributions. The pdf of Nakagami distribution describes the received envelope by a central chi-square distribution, $\Gamma(m)$, with m degree written as:

$$f_R(r) = \frac{2m^m r^{(2m-1)}}{\Gamma(m)\Omega_p^m} \exp\left(\frac{-mr^2}{\Omega_p}\right) \qquad (r \geq 0, m \geq 1/2) \tag{2.15}$$

where Ω_p and m denote the average power and model parameter, respectively. By varying the value of m, the model can capture various distributions. For $m = 1$, the model converges to

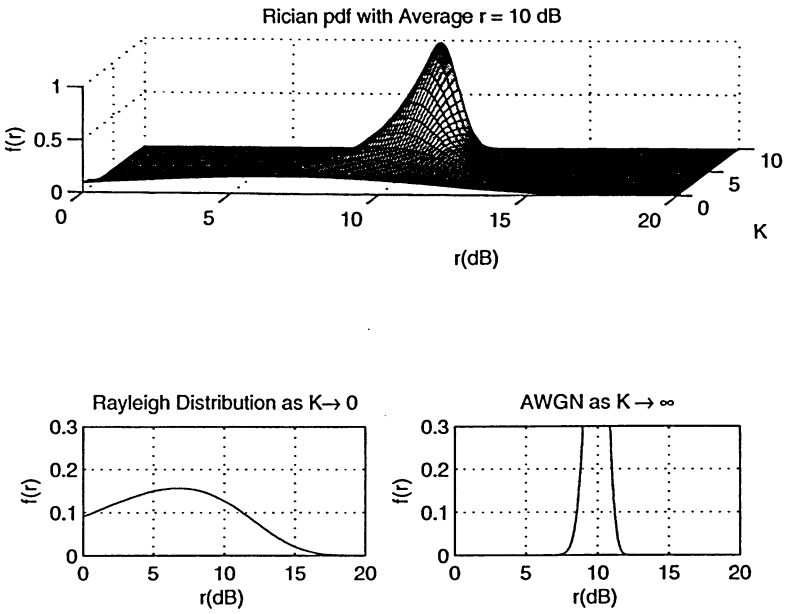

Figure 2.4: pdf of Rician Distribution

Rayleigh fading model. Setting $m = 1/2$ makes it a one sided Gaussian distribution. While setting $m \rightarrow \infty$ transforms it into a "no-fading" model. Finally, the Rician distribution can be approximated through the Nakagami model using the following relationship give by:

$$m = (K+1)^2/(2K+1) \tag{2.16}$$

Fig. 2.5 plots the pdf of Nakagami-m distribution.

2.2.5 Suzuki Process Model

The Suzuki model is a statistical model that has been developed for the land radio channel on the assumption that the local mean of the Rayleigh process follows a log-normal statistic and accounts therefore for the effects caused by shadowing [39].

In urban areas, the direct LOS component between the MS and BS is for most of the time completely obstructed by high buildings. In such case, the signal at the receiver is composed of many independent reflected signal components coming from all directions in the horizontal plane. As discussed in Section 2.2.2, the envelope of the received signal is

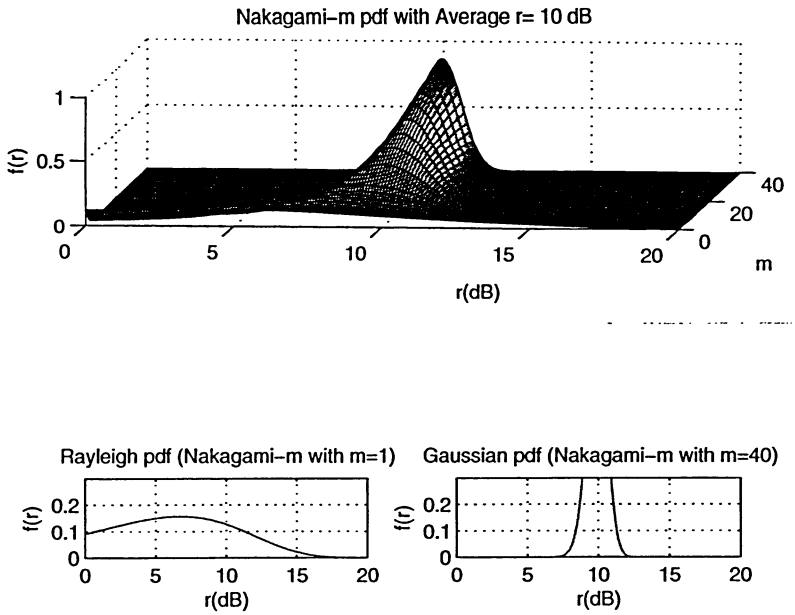

Figure 2.5: pdf of Nakagami-m Distribution

then Rayleigh distributed. If the mobile station moves a small distance, the environment characteristics can be considered as approximately constant, and therefore, the power of the Rayleigh process can also be considered as approximately constant. But for large distances, the large environment characteristics are slowly varying, and the power of the Rayleigh process can vary considerably. In this case, a Suzuki process models the stochastic process more precisely.

A stationary Suziki process $\phi(t)$ is obtained by the multiplication of a Rayleigh process $\varphi(t)$ with a log-normal process $\chi(t)$ [40] given by:

$$\phi(t) = \varphi(t) \cdot \chi(t) \tag{2.17}$$

Fig. 2.6 presents the simulated fading envelope of Rayleigh fading, shadowing and Suziki process with the parameters of mobile speed $v = 50km/h$ and carrier $f_c = 2GHz$. It can be observed that Suzuki process can catch the effect of Rayleigh process in the small scale and log-normal shadowing process in the large scale.

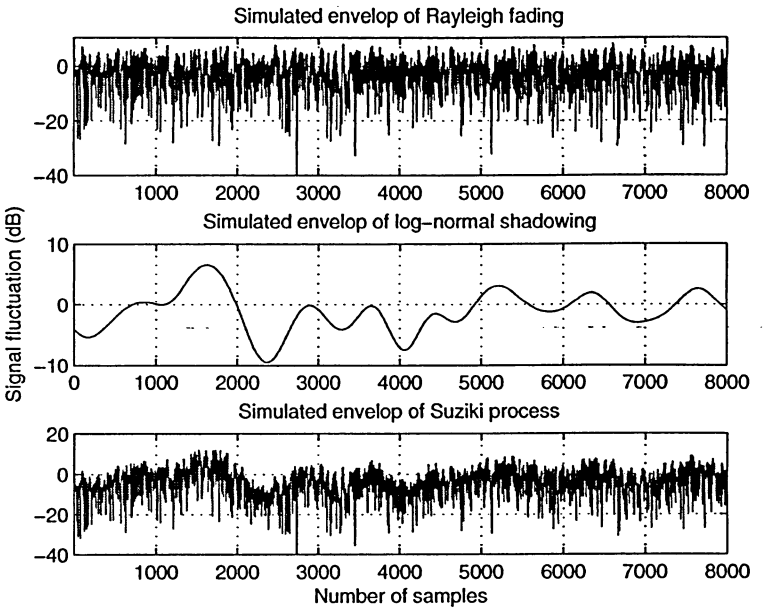

Figure 2.6: Simulated Fading Envelope: Rayleigh Fading, Log-normal Shadowing and Suzuki Process

2.3 Mitigation Techniques for Channel Fading

As discussed already, channel fading can severely degrades the system performance. Improving the quality or reducing the effective error rate in a multipath fading channel is extremely difficult. In AWGN channel, using typical modulation and coding schemes, reducing the effective bit error rate (BER) from 10^{-2} to 10^{-3} may require only 1 or 2 dB higher signal-to-noise ratio (SNR). However, it requires up to 10 dB improvement of SNR in multipath fading environment [41]. Fig. 2.7 plots the BER performance comparison between AWGN channel and fading channel as a function of SNR.

There are some mitigation techniques applied in wireless communication systems to combat the effects of channel fading, listed in Table 2.1. It indicates which technique is best suited for ameliorating the degradation due to various fading effects. The mitigation approaches to be used when designing a system should be considered into two basic steps:

- Choose the type of mitigation to reduce or remove any distortion degradation (fast

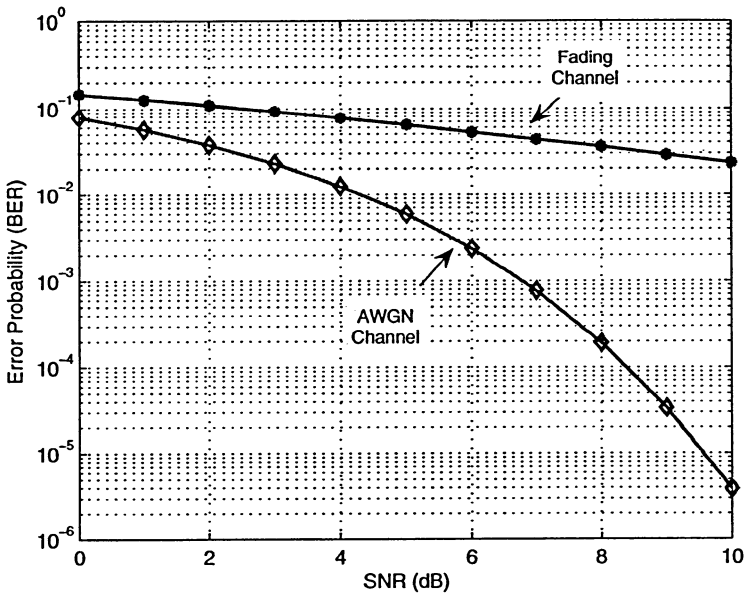

Figure 2.7: Performance of BER Degradation over Fading Channel

fading, frequency-selective fading).

- Combat the fading effects of loss in SNR (flat fading, slow fading) to approach AWGN system performance by using some forms of diversity, power control, or by using a powerful error-correction code.

Channel Fading	Mitigation Approach
Large-scale fading (near-far-effect)	Power control
Frequency-selective fading	Adaptive equalization, OFDM , Pilot signal Direct-sequence spread-spectrum (DS/SS)
Fast fading	Robust modulation, Coding and interleaving
Flat fading	Diversity technique, Power control
Slow fading	Error-correction coding

Table 2.1: Mitigation Techniques for Channel Fading

It is well known that power control is one of the most widely used mitigation techniques to compensate for the loss caused by propagation and fading. Furthermore, it is an efficient

technique to alleviate the multiple access interference in CDMA systems, as will be discussed in the following chapters.

Chapter 3

Combined Power Control and Rate Adaptation Techniques

The effective radio resource management (RRM) is essential to the success of the wireless networks. The aim of RRM is to efficiently utilize the limited radio resources and to provide more mobile users with the guaranteed quality of service (QoS). The RRM contains many sub-blocks such as the connection admission controller, the traffic classifier, the radio resource scheduler, and the interference and noise measurement [42]. Mobile station's transmission power and date rate are two important radio resources which should be well controlled to achieve different objectives like maximizing the number of simultaneous users, reducing the total transmitting power, and increasing the total throughput. The conventional approach to achieve these objectives is to select one of them as an objective function to optimize under some constraint conditions.

Shannon's channel capacity equation is given by

$$C = \frac{1}{2}\log_2(1 + CIR). \tag{3.1}$$

It shows that the information rate related to the channel capacity (C) is an increasing function in CIR. Increasing the information rate is generally very desirable in data communication systems but it is restricted by the CIR. Increasing the CIR can be achieved in two ways. The first way is by reducing the total interference and noise affected by that user. This depends on some characteristics of the noise and the interference. If the users concurrently use the

channel, such as in DS-CDMA, then the interference can be reduced by using power control techniques. The second way of increasing the CIR is simply by increasing the transmission power. In a single user communication system (point to point) or in broadcasting, this can be an acceptable solution and the main disadvantages are the cost and the nonlinearities in the power amplifiers. But in multi-user communication environment, increasing the transmission power means more co-channel and cross-channel interference problem. Thus, power control is an essential mechanism to deal with this problem.

Controlling the data rate as well as controlling the transmission power is an important topic in modern communication systems. The adaptive rate feature are not needed for communication systems which are designed mainly for voice communication as in 1G and 2G cellular systems. In these systems, the target CIR is specified, and the data rate is fixed and only the power is controlled, such as in IS-95. While the 2.5G/3G mobile cellular systems are supporting the multi-rate data communication because they are designed not only for voice service but also for data and multimedia services. An efficient combining algorithm for power and rate control is required for these systems. We address the problem in this chapter as how to combine both the power and rate in an optimum way to meet the required specifications. Section 3.1 and section 3.2 will give a detailed overview of power control and rate adaptation techniques, respectively. A novel combined power control and rate assignment algorithm is proposed in section 3.3.

3.1 Power Control in CDMA Systems

In a CDMA system, all users are sharing one radio channel and multiple access is achieved through the use of a specific spread spectrum pseudonoise code for each user. System performance is very much dependent on multiple access interference (MAI) which is caused by the crosscorrelations between the desired user's signal and other users' signals. Power control is employed to keep the CIR nearly constant at a desired level and achieve the optimum capacity, thus enhancing the system performance.

Power control (PC) serves as an integrated role in CDMA systems: *power allocation*,

also called slow power control, and *Closed loop power control* (CLPC), also called fast power control. Power allocation is an important resource management function for multiclass systems, see for example, [43, 44, 45], and the references cited in. In these systems, power allocation is used to specify the target received power levels. It is applied as a control knob to satisfy the Quality of Service (QoS) requirement and peak power restrictions of all the users in the system. On the other hand, target power level definition along is not sufficient for a wireless environment, where signals experience path loss, fading and shadowing. As a result, transmit power control is used to compensate the signal impairment to make the received signal strength (or CIR level) to maintain at the target level. More details about the classification of transmit power control will be given in Section 3.1.2.

3.1.1 Near-far Effect

Consider the situation depicted in Fig. 3.1. Mobile stations MS_1 and MS_2 share the same frequency band and their signals are separable at the base station by their unique spreading codes. The link attenuation of MS_2 at a particular time instance might be much greater than that from MS_1 to BS. If power control is not applied, the signal of MS_1 will overpower the signal of MS_2 at the base station. This is so-called *near-far effect.* To alleviate this effect, power control aims to set the transmission power of MS_1 and MS_2 so that both signals are received at the same mean power level at the BS.

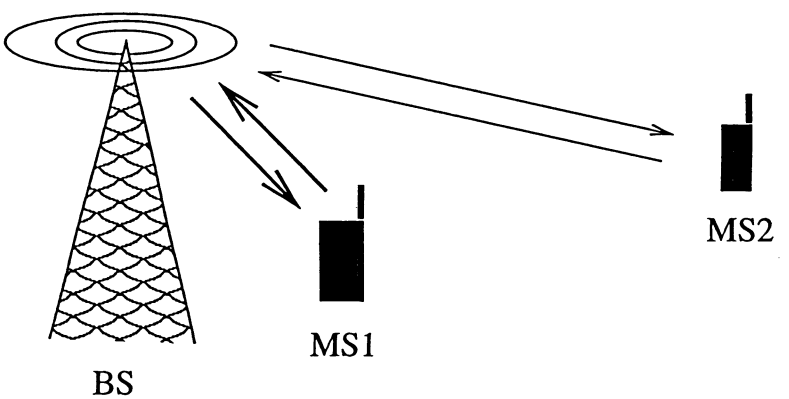

Figure 3.1: Near-far Effect

As can be understood from the discussions in section 2.2.1, the received signal power attenuation is a random variable and the variation of the received signal strength about the local mean value is called fading. Both of fading and the *near-far effect* cause the degradation of the system capacity in CDMA systems. While an efficient power control scheme can be applied to reduce the variations of the received power and increase the system capacity.

3.1.2 Classification of Power Control Techniques

Power control can be classified in many different ways, as shown in Fig. 3.2

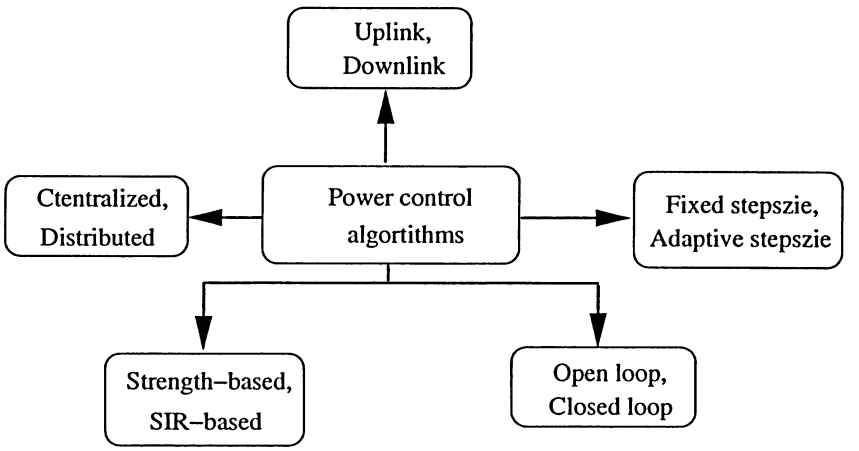

Figure 3.2: Classification of Power Control Techniques

- *Centralized and distributed power control*:

The centralized power control, see e.g. [46, 47, 48] requires a central controller which has all information about the established connections and channel gains, and controls all the power levels in the network or part of the network. The feasible power solution can be found when the maximum eigenvalue of the power matrix is less than 1. The central idea in power control schemes is to maximize the minimum CIR in each of the channels in the system. However, the centralized power control is not easy to implement in practice. And it can be used to give bounds on the performance of the distributed algorithms.

The distributed power control algorithm depends only on local information, such as measured CIR or channel gain of the specific user, see e.g. [49, 50, 51]. These algorithms perform well in rather ideal cases, but in real systems there are a number of undesired effects, such as [28]:

1) Measuring and control signaling take time, which results in time delays in the system.

2) The signals needed for control may not be available and have to be estimated.

3) Quality is a subjective measure, and relevant objective measures have to be employed.

- *Strength-based, SIR-based power control*:

From the decision-making criteria standpoint, power control methods can further be grouped into strength-based see e.g. [52] and SIR-based, see e.g. [53, 54]. In strength-based power control scheme, the strength of a received signal at the base station from a mobile is measured to determine whether it is higher or lower than the desired strength. These algorithms typically adjust the transmission powers inversely proportional to the link gain. In SIR-based scheme, the measured quantity is based on SIR (signal-to-interference ratio) where interference consists of channel noise and multi-user interference. It is know SIR can be calculated after the signal despreading in CDMA systems.

A problem associated with SIR-based power control is the potential to get positive feedback to endanger the stability of the system. Positive feedback arises in a situation when one mobile station under instructions from the base station has to raise its transmission power in order to deliver a desirable SIR to the BS, but the increase in its power also results in an increase in interference to other users so that these other mobile users are then forced to also increase their power, *etc.*

In [53, 54], it has been shown that SIR-based power control offers better performance, such as QoS and system capacity, than strength-based algorithms. While strength-based power control is easier to implement. In addition, a combined strength-based and SIR-based power control algorithm was proposed in [55] and reported to perform better than plain SIR-based power control.

- *Open loop and closed loop power control*:

Open loop power control mitigates the path loss and large-scale variations such as shadowing. In this case, the mobile users adjust their power levels on the basis of the received power of a pilot signal broadcast by the base station from the forward link direction. Thus, the open loop power control scheme is employed for the initial power setting. However, it is not possible to compensate multipath fading by using open loop power control because uplink and downlink are not correlated.

Closed loop power control is applied to eliminate variations due to multipath fading by using feedback information, so as to achieve the desired QoS. It consists of *inner-loop* and *outer-loop* components. The *inner-loop* involves one-bit feedback from the base station to the mobile unit to lower or raise the power by δ dB, depending on the difference between the measured CIR value and the target CIR. While *outer-loop* is used for target CIR adjustment. It is based on BER and frame error rate (FER) measurements and its role is to change the target CIR when the situation of mobile is changing for the power control planning. Thus, an *outer-loop* varies the target CIR as a function of FER [24]. A typical way to do this in practice is to raise the target by a larger step δ_{up} when a frame is discard, and to decrease the target with a smaller step δ_{down} when a frame is correctly received [56]. In [57], another *outer-loop* power control algorithm was proposed which was able to detect changes in the multipath channel profile and compensate for errors in the mapping between FER and CIR target, yielding faster tracking of the channel changes.

- *Fixed stepsize and adaptive stepsize power control*:

According to power update strategies, CLPC can be performed by using fixed stepsize power control (FSPC) algorithm, see e.g. [12, 58] and adaptive stepsize power control (ASPC) algorithm, see e.g. [24, 59]. Power control in fixed stepsize algorithm is a simple 1-bit power control command (PCC). Based on the PCC received from the base station, the transmission power of mobile station is either increased (PCC="+1") or decreased (PCC="-1") by the fixed stepsize to 1 dB in the conventional closed loop method. While a specific example of the ASPC algorithm increases or decreases the mobile station's transmission power depending on power control command (PCC) history and the Doppler frequency [59]. In

[24], it was shown that the variable stepsize is a function of the current and past *PCC* bits. If the base station detects the same *PCC* from a mobile in a set of consecutive slots, the stepsize dedicated to the mobile is increased. On the contrary, if an alternative sequence of up and down *PCCs* of a mobile are received by a base station, the stepsize dedicated to this mobile is reduced. It has been shown that the ASPC algorithm is superior to the FSPC algorithm, while the fixed stepsize algorithm is easier to implement.

- *Uplink and downlink power control*:

Power control can also be employed at uplink and downlink. It is well known that power control for CDMA systems is more crucial and sensitive on the uplink in the sense that power levels received at the base station from different mobile stations should be roughly equal. In this case, it is necessary to have a dynamic range for control on the order of 80 dB [28].

In downlink the situation is different, since all signals transmitted by a base station propagate through the same radio channel before reaching a mobile station. Therefore, since they undergo the same attenuation, power control is not needed for *near-far* problem. Instead, power control is used to provide more power to users located near the cell borders, suffering from high interference from nearby cells and, on the other hand, to use only sufficient transmission powers in order to minimize the interference produced to nearby cells [29]. In principle, the downlink signals to different users could be made orthogonal by using proper spreading codes. Unfortunately, the orthogonality of the downlink signals is lost in practice due to multipath propagation. Therefore, allocating different powers for different users in downlink could cause a *near-far* situation at the mobile stations. For this reason, the dynamic range of downlink power control is usually much smaller than that in uplink, typically of 20-30 dB [60].

The focus in this thesis is on uplink power control, although the proposed algorithms could also be applied to downlink power control.

3.1.3 Uplink Power Control Model

The task of uplink power control is to vary users' transmission powers in order to compensate for the channel variations with desired power level at the base station. The algorithms proposed in this thesis are targeted to improve the transmit power control performance and is done using the combination of open loop, closed loop and outer loop power control schemes. In the closed loop power control in the uplink, the base station needs to set target CIR to maintain the reliable QoS for all the mobile stations. Measuring the received CIR of a mobile station and comparing it with the target CIR^*, the based station decides and sends a PCC over the feedback channel.

The UMTS W-CDMA system defines the variable stepsize for the power control algorithm. While the conventional closed loop power control algorithm employed in IS-95 systems is a fixed stepsize power control (FSPC) algorithm. This type of algorithm has been presented in [61] give by:

$$P_i(t+1)_{(dB)} = P_i(t)_{(dB)} + \delta_{(dB)} \cdot PCC(t) \tag{3.2}$$

$$PCC(t) = sign(\xi_i^* - \xi_i(t)) \tag{3.3}$$

where $P_i(t)$, ξ_i^* and $\xi_i(t)$ represent the transmission power, the target CIR^* and the measured (received) CIR, respectively, of the ith user at the tth time slot. δ is the applied stepsize. The Power Control Command (PCC) of a "+1" or a "-1"" is obtained by:

$$sign(x) = \begin{cases} +1 & \xi_i < \xi_i^* \\ -1 & \xi_i > \xi_i^* \end{cases} \tag{3.4}$$

Typical TPC updates are from 800Hz (used in the IS-95 system [13]) to 1500Hz (used in W-CDMA [5]). Note that the update rate cannot be arbitrarily high because of the inherent delay and control overhead imposed by the CIR measurement process.

The uplink power control system model is illustrated in Fig. 3.3. At the time t, the base station measures the uplink CIR. This measurement can be written as

$$\xi(t) = P(t-1) + g(t) - I(t) \tag{3.5}$$

where $g(t)$ and $I(t)$ are the channel attenuation and the total interference power at time t, all in decibels. The measurement is compared to the uplink target CIR^* set by the outer loop control. Based on this comparison, the BS sends a command $PCC(t)$ to the MS over a feedback channel either increasing or decreasing its power by a fixed stepsize, typically 1 dB. The command is transmitted to the MS uncoded to reducing processing delays, for which reason the command bit error probability can be relatively high, e.g., up to 10%. The mobile station receives the command $PCC(t)$ and update its transmission power correspondingly.

Besides, the loop delay (feedback delay) in this model refers to the overall loop delay in closed loop power control. It greatly affects the performance of the power control algorithm. This delay is a combination of the delays due to the CIR measurement process, the transmission of the CIR information over the radio channel, the processing of the CIR information and the adjust of the transmission power. Therefore the power update is based on the outdated information of the received CIR. This may cause instability in the power control algorithm, leading to large variations in the interference powers at the receivers and diminishing capacity.

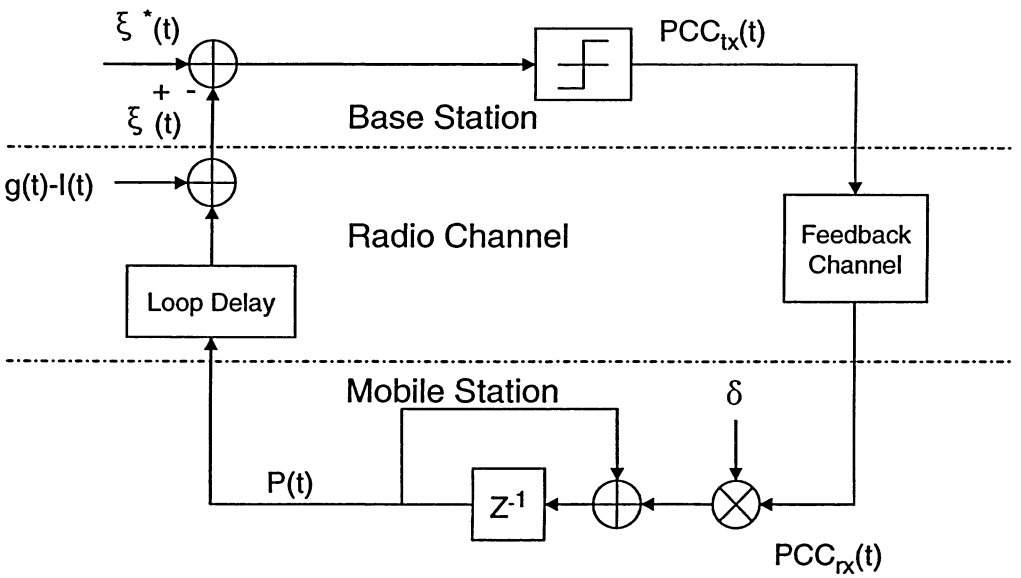

Figure 3.3: Block Diagram of Uplink Closed Loop Power Control

3.1.4 Quality Measures for Power Control

A great deal of the work on power control in CDMA cellular systems has focused on how to set the transmission powers so that all the users in the system have acceptable *energy-to-interference-spectral-density ratio* (E_b/I_o) where I_o is spectral density from both the multiple access interference (MAI) and background noise. This approach is based on the fairly reasonable assumption that the BER probability at the receiver is a strictly monotonically decreasing function of E_b/I_o. For instance, BER P_b of binary phase shift key (BPSK) modulation in an AWGN channel is given by [31]

$$P_b = Q\left(\sqrt{\frac{2E_b}{I_o}}\right), \tag{3.6}$$

where $Q(x)$ is defined by

$$Q(x) = \frac{1}{\sqrt{2\pi}} \int_x^\infty e^{-t^2/2} dt, x \geq 0 \tag{3.7}$$

A more relevant case for CDMA cellular system is the average BER performance of RAKE receiver in fading channels. Assuming binary modulation, Rayleigh fading channel, the average BER at the output of RAKE receiver using MRC is given by [62]

$$\bar{P}_b = \int_0^\infty Q\left(\sqrt{\frac{2E_b}{I_o}}\right) \cdot f_{\frac{E_b}{I_o}}(\gamma) d\gamma \tag{3.8}$$

where γ represents the instantaneous SNR per bit of each branch. Let Γ=E_b/I_o which denotes the average value of γ. Thus Eq. (3.8) can be written as

$$\bar{P}_b = \int_0^\infty Q\left(\sqrt{2\Gamma}\right) \cdot f_\Gamma(\gamma) d\gamma \tag{3.9}$$

Besides, E_b/I_o is also called signal-to-interference ratio (SIR) which is calculated after signal despreading at the receiver in CDMA systems and closely related with another measure, namely the CIR calculated before despreading and denoted by ξ, such that

$$E_b/I_o = \xi \cdot \frac{W}{R} \tag{3.10}$$

where W is the transmission bandwidth in Hz and R is the data rate. The W/R is called *processing gain*, denoted by G [29]. It can be seen that the difference between the E_b/I_o (or SIR) and CIR is the processing gain G (*i.e.*, SIR = CIR $\times$ G). When the data rate is fixed, the CIR differs from E_b/I_o by merely a scale factor.

3.2 Transmission Rate Control

The current DS-CDMA digital cellular networks have been primarily designed to support voice traffic. However, the next generation wireless communication networks (3G mobile communication system) are expected to support traffic with diverse bandwidth (multi-rate) requirement. Multi-rate wireless system are fairly new and a full understanding of how to perform rate control efficiently in practice is not available. Some research work has been conducted to gain better understanding of rate assignment. Implementation is not the main concern in these research papers and their focus is theoretical.

Most work studied the rate assignment for the purpose to maximize the system throughput, see e.g.,[63, 64, 65]. In [63], the optimal solution suggests that MS that has a better channel condition should transmit a higher data rate than others that experience worse channel conditions. The study in [63] did not consider the maximum allowable load, which is indicated by the interference in each cell. In [64], system throughput maximization with the constraint of a certain peak interference level was investigated. Only a group of MSs that have good channel conditions can transmit data and the remaining have to delay the transmission. Most of the MSs that are allowed transmit data are assigned the maximum power and rate. Both [63] and [64] show that system throughput maximization can lead to fairness issues.

3.2.1 Multi-rate Transmission Schemes

W-CDMA technology, which is the major radio transmission scheme for the UMTS, has intrinsic support for dynamic rate transmission [5]. The understanding idea is that it supports to use variable spreading gain, where users are allowed to transmit different data rates in fixed-length time frames and multi-code techniques as well. There are main three ways in which a particular information rate can be achieved.

- *The variable-spreading gain (VSG) scheme*:

In a variable-spreading gain scheme, the chip rate is constant across mobile users, but the spreading gain may be different. Each mobile's processing gain (PG), G, is determined as the ratio of the common chip rate (R_c), or equivalently the bandwidth (W), see Eq. (3.10), to the mobile's bit rate, written as

$$G = \frac{R_c}{R} \tag{3.11}$$

Adaptive rate allocation schemes in terms of PG were investigated in [16, 63, 66] and proven to be an efficient way to obtain high link throughput.

In UMTS, the VSG scheme is called orthogonal variable spreading factor (OVSF) scheme, where the chip rate is fixed at a specified value (4.096 Mcps for W-CDMA) and the data rate can take different values. This means that the PG is variable. The PG can be defined as the number of chips per symbol. In UMTS, the processing gain (or the spreading factor) in the uplink can take one of the following values, e.g. {4, 8, 16, 32, 64, 128, 256}. Thus the physical channel bit rate varies in the range of 32-2048 kb/s [67].

- *Multi-code (MC) scheme*:

In MC-CDMA systems, all the data signals over the radio channel are transmitted at a basic rate, R_b. Any connection can only transmit at rates $m \cdot R_b$, referred to as $m-$rate, where m is a positive integer. When a user needs to transmit at $m-$rate, it converts its data stream, serial-to-parallel, into basic-rate streams. Then each stream is spread by using different and orthogonal codes. The set of codes available to each user are orthogonal within themselves. Multi-code scheme has almost the same performance as VSG scheme. However, it suffers from the disadvantage of a high peak-to-mean envelope power ratio [68]. The orthogonality of codes is also compromised in frequency selective fading [63].

- *Multi-level modulations scheme*:

From Eq. (3.11), it is noted that decreasing processing gain will increase the data rate. When PG is at the minimum value, users can further adjust the transmission rate by using higher order of quadrature amplitude modulation (QAM) constellation if the requirement of

BER performance can still be fulfilled, see e.g. [18]. However, this scheme has significantly worse performance for high rate users [63].

Based on above discussions, we restrict out attention to the multiple processing gain scheme for the multi-rate transmission in this thesis.

3.2.2 Discrete Transmission Rate and CIR Relation

In order to assign the data rates, one possibility is to relate them to target $CIRs^*$. We may then for example assume access to infinitely many target $CIRs^*$, resulting in a continuous relation between transmission rate and CIR. If instead the number is limited, it becomes a discrete relation. In Fig. 3.4, an example of a linear and a discrete relation between the effective data rate and CIR is depicted.

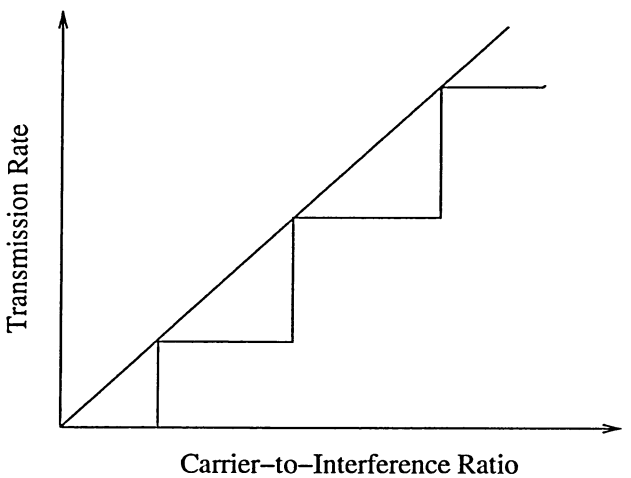

Figure 3.4: An Example Illustrating a Continuous Linear and Discrete Transmission Rate and CIR Relation

A linear relation is motivated in DS-CDMA systems where the processing gain is adapted by the symbol duration and also the fact that the rate in wideband Gaussian channels is approximately linear. With adaptive modulation and coding, a linear growth can be too optimistic and a logarithmic mapping is often used. An immediate interpretation of the assumption of a relation between rate and target CIR^*, is a guaranteed maximum BER. If the connection is established at a certain CIR, say the predetermined target, it can be

assumed that there exists a one-to-one relation to a corresponding bit error probability. This, by choosing the proper target $CIRs^*$, the data rate can be offered with a specified bit error probability. In particular for a DS-CDMA system, a high target CIR^* compensates for the low processing gain when using a high data rate. Thus, it is a key issue to design algorithms that assign the proper target $CIRs^*$ and data rates to users in a multi-rate transmission system.

3.3 Combined Power Control and Rate Adaptation

Power control and rate assignments affect both QoS and radio resource utilization in mobile data networks. With the increasing demand of wireless communications, how to improve transmission efficiency has attracted lots of research attention in recent years. In particular, the subject of the combined power control and rate adaptation techniques in DS-CDMA networks has attracted considerable research interest. In [69] and [70], the joint power control and rate adaptation scheme where the mobile transmission power was well controlled based on the target CIR level was employed to achieve the maximum throughput. Ulukus *et al.* [71] implemented a "snap-shot" evaluation approach where the authors assumed that the adaptation convergence much faster compared to the changes in the channel gains. A single user water-filling strategy was proposed in [18] where the user with better channel condition would be assigned less power. As a result, the transmission power was distributed according to the mobile user's individual instantaneous channel condition. Li *et al.*[72] developed a framework of utility-based joint power control and rate allocation scheme for downlink CDMA systems employing either matched-filter or blind multiuser receivers. The rate and power control algorithms made use of the recent analytical results on the SIR performance of the blind multiuser detector. The distributed strategies for the joint control of power and data rates by taking into account the network congestion levels were proposed in [73]. The design was pursued by formulating state-space models with and without uncertain dynamics and by determining control signals that helped meet certain performance criteria (such as robustness and desired levels of SIR). In [74], the author examined the joint

optimization of outer-loop power control and transmission rate adaptation, to maximize the spectral efficiency, subject to a long-term transmit power constraint. The proposed adaptive transmission scheme in which the target SIR and data rate were adapted to the estimated BER while a constant short-term received SIR was maintained by exploiting total or truncated channel inversion strategy in the inner-loop power control, was analyzed and simulated for the multi-QAM modulation scheme over flat fading channel. In [75], the algorithm of the combined power and rate adaptation was presented, where the optimal spreading factor allocation criterion was applied to maximize the throughput.

In this section, we are interested in developing a novel joint power and rate allocation algorithm [1]. The greedy rate packing (GRP) [27] allocation scheme is applied in the rate adaptation. The GRP assigns a higher transmission rate to the users with better channel conditions (higher channel gain) meanwhile minimizing the transmission power based on the power constraints. It can be interpreted that more resources, like power and transmission rate, are allocated at time instants when channel conditions are favorable. The link which is in deep fading will be assigned lower rate, or even be turned off when fading is lower than a predefined threshold. As a result, the resource allocation will be working in an efficient way.

3.3.1 System Model

We consider a single cell W-CDMA system supporting delay-tolerant service containing N users, as shown in Fig. 3.5. Each user can transmit with a power in the range $P_{min} \leq P_i \leq P_{max}$. The data rate of each user can be different in order to adapt to channel conditions. Besides, the signals of all users are spreading to the same bandwidth W, and only uplink (MS to BS) is concerned in this work. The propagation loss due to effects of shadowing and multipath fading are captured by the link gain, while the path loss effect is neglected here.

Furthermore, we use a land mobile radio channel model for urban areas, where the fading effects define that the small-scale fading is being superimposed on the large-scale fading in our system. For such a channel model, we use Suzuki process $\phi(t)$ which is obtained by the multiplication of a Rayleigh process $\varphi(t)$ with a log-normal process $\chi(t)$ [40] shown as:

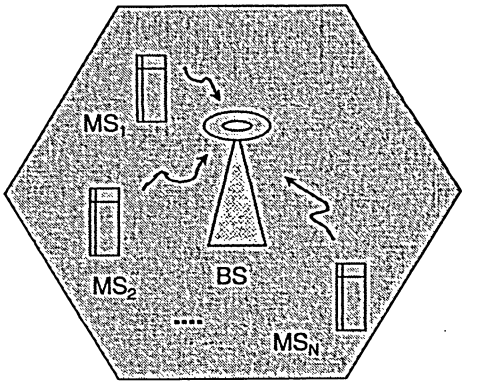

Figure 3.5: A Single Cell with N Active Users

$\phi(t) = \varphi(t) \cdot \chi(t)$. As discussed in Section 2.2.5, Suzuki process can catch the effect of Rayleigh process in the small scale and log-normal shadowing process in the large scale. The reason we define the Suzuki process as our channel model is that: the Suzuki process models the stochastic process more precisely than the Rayleigh process in the urban areas, where the direct-line-of-sight component between the mobile user and base station is for most of the time completely obstructed by high buildings [40]. For simplicity, the power of the Rayleigh process is considered to be constant when the mobile station moves a small distance. However, for the large distances (urban environment), the environment characteristics are slowly varying, and the Suzuki process is more suitable.

The system capacity and many other QoS measures, including BER, channel efficiency and throughput, depend on the received E_b/I_0. For a single cell system, the expression of E_b/I_0 of the ith user is given by

$$\left(\frac{E_b}{I_0}\right)_i = \frac{W}{R_i} \cdot \xi_i = G_i \cdot \xi_i \tag{3.12}$$

where $G_i = \frac{W}{R_i}$ is the spreading gain and ξ_i denotes the CIR given as

$$\xi_i = \frac{P_i h_i}{\sum_{j \neq i} P_j h_j + \eta_0} \tag{3.13}$$

where P_i and h_i denote the transmission power of the ith user and link gain, respectively. The term η_0 is the average power of the background noise.

In addition, each user i can be assigned a discrete rate from the set $\mathbf{R} = \{0, r^{(1)}, r^{(2)}, \cdots, r^{(k)}\}$, with the condition, $0 < r^{(1)} < r^{(2)} < \cdots < r^{(k)}$, and therefore, a different spreading gain G_i. The objective is to assign a higher data rate to the users in good channel condition to enhance throughput and to allocate a lower data rate (and correspondingly, a larger spreading gain) to the users in bad channel condition to protect the transmitted message. On the other hand, CIR is another mechanism to match the effective data rate. We predefine a set of discrete target CIR^*s, $\Omega = \{0, \xi^{(1)*}, \xi^{(2)*} \cdots \xi^{(k)*}\}$, and with the condition, $0 < \xi^{(1)*} < \xi^{(2)*} < \cdots < \xi^{(k)*}$, where k is the number of available rate which the users can be assigned. Moreover, we assume a common target $(E_b/I_0)^*$ being fixed for all users. Thus, the relationship between these two mechanisms can be obtained from Eq. (3.12) shown as:

$$\frac{r^{(1)}}{\xi^{(1)*}} = \frac{r^{(2)}}{\xi^{(2)*}} = \cdots = \frac{r^{(k)}}{\xi^{(k)*}} = \frac{W}{\left(\frac{E_b}{I_0}\right)^*} \tag{3.14}$$

It can be seen from Eq. (3.14) that each target CIR^* corresponds to each rate. As a result, the rate assignment and target CIR^* assignment are interchangeable.

As mentioned in Section 1.2.2, the transmission unit in the UMTS W-CDMA interface is a 10 ms frame. Each frame is divided into 15 time slots and each slot contains one power control command (PCC). Therefore, the transmission power is updated slot by slot, while the data rate is updated frame by frame.

On the basis of the system and channel model discussed above, our goal is to maximize the total throughput of the system averaged over the fading distributions of mobile users. Since the effective transmission rate and QoS objective are closely related to the CIR, which can be efficiently controlled by CIR-based power control, it becomes natural to investigate a joint scheme for rate and power adaptation. Besides, we also attempt to save average transmission power consumption for every mobile user as well, by using combined power control and rate adaptation scheme.

Closed loop power control (CLPC) regulates the received power around the target level and makes the transmit power tracking the time-varying channel to compensate the channel impairments. Consequently, our aim is to suggest an integrated rate assignment (by

using GRP) and power control algorithm which will offer high throughput with low power consumption.

3.3.2 Dynamic Power Control and Rate Assignment Algorithm

We develop a combined power and rate allocation scheme in a VSG-WCDMA system. We first reassign the target $CIR^*(\xi^*)$ to every mobile user based on its channel condition, then the data rate will be allocated to every mobile user from a finite set of discrete transmission rates, $\mathbf{R}$. After the target CIR^* and rates being assigned, the transmission power adaptation of each mobile user can be employed by using closed loop power control in the range $P_{min} \leq P_i \leq P_{max}$. This solution minimizes the total power consumption and maximizes the data rates to the users under the power constraints. In addition, we also extend our approach to a frame/time slot structure of W-CDMA systems.

- ***Rate assignment***:

As mentioned before, we apply the GRP [27] algorithm to allocate the data rate, and correspondingly, the target CIR^*, of the users with the aid of their channel state information. It should be noted that the channel information and the received CIR are considered to be well estimated at the BS. Thus, the GRP algorithm maximizes the throughput by judicious allocating the data rate to each user.

Assume channel gains of every user are sorted in a decreasing order: $h_1 \geq h_2 \geq \cdots \geq h_N$. Based on Eq. (3.14), there exists a feasible target CIR^* assignment which minimizes the total power, such that $\xi_1^* \geq \xi_2^* \geq \cdots \geq \xi_N^*$. The target CIR^* of every user can be reassigned in terms of N constraints given by [76]

$$\sum_{j=1}^{N} \frac{\xi_j}{1+\xi_j} \leq 1 - \max_{1 \leq j \leq N} \left[\frac{\frac{\xi_j}{1+\xi_j}}{\frac{h_j P_{max}}{\eta_0}} \right] \tag{3.15}$$

where η_0 represents the background noise power. From (3.14), it can be derived that $r_1 \geq r_2 \geq \cdots \geq r_N$. As a result, the rate of the ith user can be assigned associated with the assigned

target CIR^* (ξ_i^*) under the constraints (3.15), given by

$$r_i^* = \xi_i^* \cdot \frac{W}{\left(\frac{E_b}{I_0}\right)^*} \tag{3.16}$$

From (3.14) and (3.16), it is clear that the user with good channel condition (higher channel gain) will be assigned higher data rate.

- ***Power control procedure***:

As discussed in Section 3.1, power control serves as an integrated role in CDMA systems: *power allocation* and *closed loop power control* (CLPC). Power allocation is an important resource management function for multiclass systems and is used to specify the target received power levels to satisfy the QoS requirement and peak power restrictions of all the users in the system. While CLPC is to compensate for the signal impairment to make the received signal strength (or CIR level) to maintain at the target level.

With a certain target CIR^* (ξ_i^*) assignment, we can find the power vector that supports every user with the minimum power by solving the linear inequalities

$$\begin{cases} (\mathbf{I} - \mathbf{F})\mathbf{P}^* \geq \mathbf{U} \\ \mathbf{P}^* \geq \mathbf{0} \end{cases} \tag{3.17}$$

where $\mathbf{P}^* = [P_1^*, P_2^*, \cdots, P_N^*]^T$ is the vector of the transmission powers,

$$\mathbf{U} = \left[\frac{\xi_1\eta_1}{h_1}, \frac{\xi_2\eta_2}{h_2}, \cdots, \frac{\xi_n\eta_n}{h_n}\right]^T \tag{3.18}$$

is the normalized noise power vector. η_i and h_i represent the ith user's background noise and channel gain, respectively. $\mathbf{I}$ is the $n \times n$ identity matrix, and $\mathbf{F}$ denotes the normalized cross-link gain matrix with (i, j) entry written by

$$F_{ij} = \begin{cases} \frac{\xi_i h_j}{h_i} & i \neq j \\ 0 & i = j \end{cases} \tag{3.19}$$

Through the manipulation of (3.17) and (3.18), the feasible minimum power solution of the ith user is obtained by

$$P_i^* = \frac{\eta_0}{1 - \sum_{j=1}^{N} \frac{\xi_j^*}{1+\xi_j^*}} \frac{\xi_i^*}{h_i(1+\xi_i^*)} \tag{3.20}$$

After BS assigns the target CIR^*, rates and initial optimal powers to the users, the closed loop power control (CLPC) starts based on the received CIR ($CIR(t)$) and the target CIR^* (ξ_i^*), give by

$$P_i(t+1) = P_i(t) + \delta \cdot PCC(t) \tag{3.21}$$

$$PCC(t) = sign(\xi_i^* - CIR(t)) \tag{3.22}$$

where δ and $PCC(t)$ are stepsize and the power control command at tth time slot, respectively. Furthermore, the updated transmission power is constrained by $P_{min} \leq P_i \leq P_{max}$.

- ***Proposed rate assignment and power control algorithm***:

Our proposed combined power control and rate allocation algorithm (see Fig. 3.6) can be applied in a frame/time slot structure of the VSG-WCDMA systems, where the transmission power is updated every time slot while the rate adaptation is employed frame by frame.

The algorithm is presented by the following steps:

Step 1. At the end of the nth frame, the base station computes the channel gains of every user and then sorts them in a decreasing order: $h_1 \geq h_2 \geq \cdots \geq h_N$, and initialize $\xi_i^*, i \in [1, N]$ by setting to zero.

Step 2. For $i = 1$ to N, do:

$$\xi_i^* = \max\{0, \xi^{(1)*}, \xi^{(2)*}, \cdots, \xi^{(k)*}\}$$

while satisfies the constraint Eq. (3.15). Users who are assigned $\xi_i^* = 0$ will be turned off to be inactive.

Step 3. At the beginning of the $(n+1)$th frame, the base station assigns the transmission rates to the users according to Eg. (3.16), while assigns data rate 0 to inactive users.

Step 4. At the mobile station, user's initial power at the beginning of the frame is assigned as Eq. (3.20). Then closed loop power control (CLPC) starts based on the target CIR^* (ξ_i^*) for every time slot.

Step 5. Go back to step 1 for the next adaptation cycle.

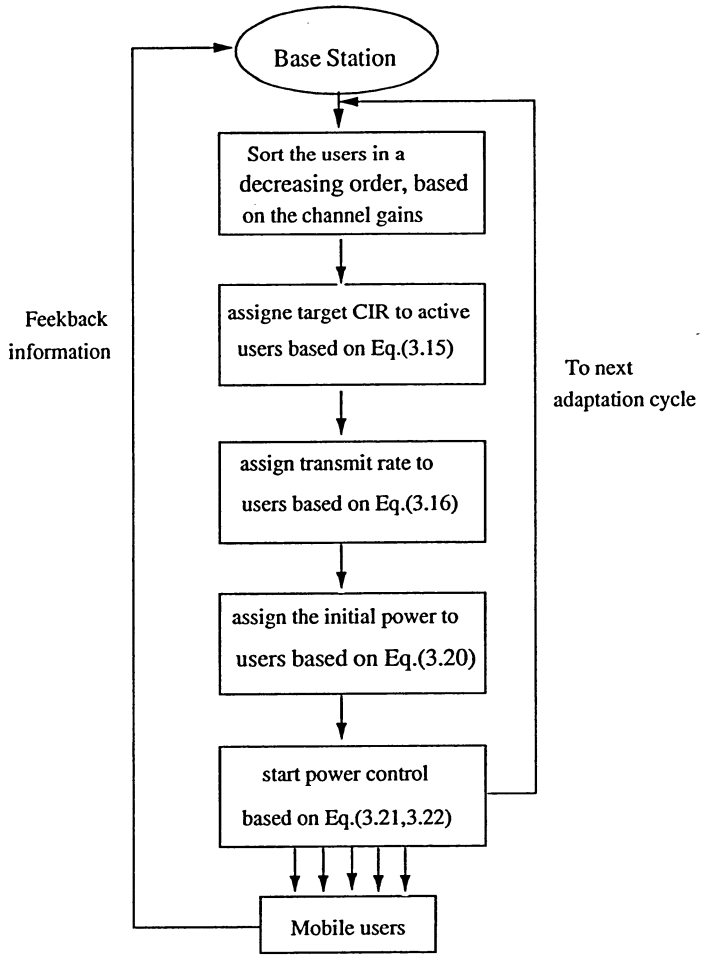

Figure 3.6: Block Diagram of the Proposed Power Control and Rate Assignment Algorithm

3.3.3 Numerical Results and Discussions

In this section, we evaluate the performance of the proposed dynamic rate assignment and power control algorithm (simply called *GRP-PC* in this section) by comparing the results of closed loop power control (CLPC) alone algorithm, rate adaptation alone scheme and another combined power control and rate adaptation algorithm called optimal spreading factor based power control (*OSF-PC*), presented in [75]. A block diagram which illustrates the rate, target CIR^* and power assignment is shown in Fig.3.7. Each source generates a sequence of fixed-length packets of length M symbol, where M is selected as 768 symbols.

The packets generated by each source enter a buffer after channel coding. The buffer contents are then converted to the DS-CDMA signal at the data rate assigned by base station. After despreading and decoding the received packet, the receiver (base station) estimates the QoS, which may be specified in terms of E_b/I_o and channel gains to reassign the target CIR^* ($\xi*$) and data rate back to mobile users. Then, the base station activates close-loop power control (CLPC) procedure.

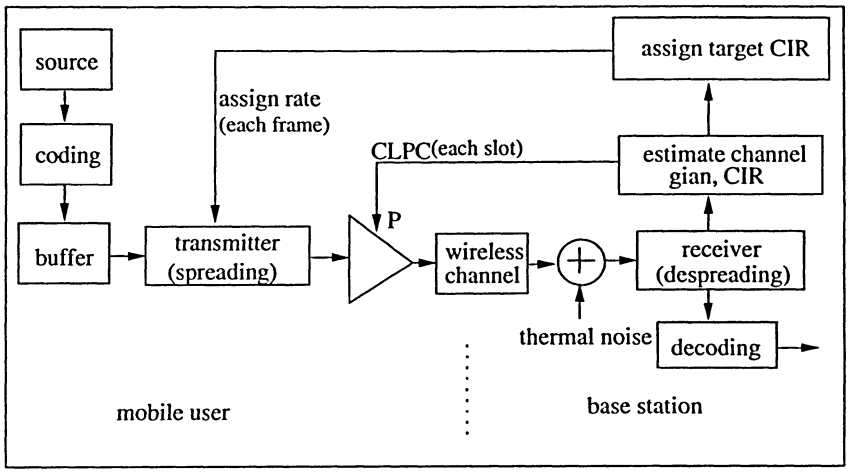

Figure 3.7: Block diagram of the simulation model

A frame/time slot structure of UMTS W-CDMA standard is employed in our simulations shown as in Fig.1.4. The chip rate and target (E_b/I_0) are assigned to 5Mchip/s and 7 dB, respectively. In addition, the mobile user speed is set from 8.1 km/h to 81 km/h. Accordingly, the normalized Doppler frequency, f_dT_p is in the range 0.01 to 0.1. The common physical layer parameters are listed in Table 3.1.

The 3G Partnership Project (3GPP) group once discussed the feasibility of attaining a $2ms$ frame length, but seems to unattainable at present [77]. Theoretically, the uplink peak transmission rate can be as high as $5.76Mbps$. However, 3GPP group has built a specification called the high-speed downlink packet data access (HSDPA) protocol that allows carriers to increase downlink throughput over W-CDMA links. 3GPP-standardized HSDPA provides a two-fold improvement in network capacity as well as data speeds up to five times (over 10

PROPERTY OF
RYERSON UNIVERSITY LIBRARY

Chip Rate (R_c)	5Mcps
Carrier Frequency	$2GHz$
Carrier bandwidth	$5MHz$
$(E_b/I_0)_{target}$	$7dB$
Fading Channel	Suzuki process
Background noise η_o	-70dBm
Frame Length	$10ms$, $2ms$
Power control frequency	$1500Hz$
Stepsize (δ)	1 dB
Number of Users	11
Number of frames	50,000
Mobile speed	$8.1km/h - 81km/h$
Power constraint	$-20dB - 60dB$
Loop delay (D)	$1T_p$

Table 3.1: Simulation Parameters of Proposed Power Control and Rate Assignment Algorithm

Mbit/s) higher than those in even the most advanced 3G networks [78]. This new technology also shortens the round-trip time between network and terminal, while reducing variances in downlink transmission delay. Those performance advances translate directly into improved network performance and higher subscriber satisfaction. HSDPA's shorter $2ms$ frame length supports a significantly reduced round trip time, which enables shorter network latency and better response time to ensure minimum delay variations. For this reason, we will use both $10ms$ and $2ms$ frame length in our simulations.

The difference between our algorithm (*GRP-PC*) and *OSF-PC* [75] is that: 1) we use GRP to assign the maximum possible data rate depending on the channel impairment which users experience. Our rate allocation scheme is based on the target CIR^* (ξ^*) reassigned to each user and the user with poor channel condition may be turned off. While the rate adaptation in *OSF-PC* works by finding an optimal spreading factor (OSF) and guarantees a minimum data rate. 2) Although both of these two algorithms use CLPC for power adaptation, we assign an initial optimal power vector, see Eq. (3.20), to users at the beginning of every frame, while *OSF-PC* initializes the power to 0 dB instead. The performance of throughput, power consumption, BER and outage probability are evaluated in this work.

In Fig. 3.8, we present the average throughput for the rate adaptation, CLPC, *OSF-PC* and our proposed rate and power adaptation algorithm (*GRP-PC*) with $10ms$ frame length. It can be observed that the average system throughput decreases when the mobile user's speed increases. It can also be observed that our proposed algorithm (*GRP-PC*) can achieve the highest average throughput compared to three other algorithms, which is about 3% better than that of *OSF-PC*, and about 5%, 24% better than that of CLPC scheme and rate adaptation scheme, respectively. Fig. 3.9 demonstrates the throughput of $2ms$ frame length simulation. It shows that the throughput is enhanced by using a shorter frame length.

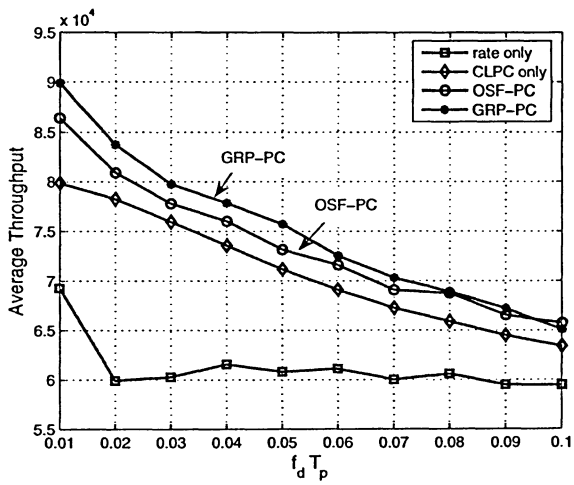

Figure 3.8: Average Throughput *vs.* f_dT_p with $10ms$ Frame Length

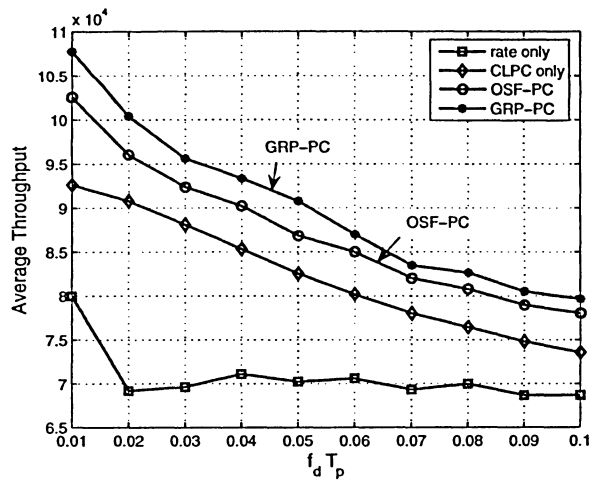

Figure 3.9: Average Throughput *vs.* f_dT_p with $2ms$ Frame Length

A comparison of the power consumption for these four adaptation approaches is displayed in Fig. 3.10 and Fig. 3.11 with $10ms$ frame length. From Fig. 3.10, it can be seen that CLPC consumes much more transmission power than other three methods in order to compensate the signal fluctuation and eliminate the variations due to channel fading. Fig. 3.11 zooms out the three low-power consumption schemes. It shows that the average transmission power of the proposed algorithm (*GRP-PC*) is a little bit higher than that of the rate adaptation while is lower than that of *OSF-PC*. The major reasons can be explained that: 1) rate adaptation tries to adapt the date rate in response to the channel fluctuation, and keeps

the transmission power fixed (set to 0dB in our simulation). As a result, it consumes the least transmission power ; 2) *OSF-PC* algorithm resets the transmission power to 0dB at the beginning of every frame, while our algorithm assigns a feasible optimal power to users based on their allocated target CIR^* (ξ_i^*). Consequently, the power consumption is reduced by applying our algorithm, which is 14% lower than that of the *OSF-PC*. It is believed that our power control scheme can work in an efficient way. Again, the lower power consumption can be observed from Fig. 3.12 by using a shorter frame length ($2ms$) compared to the case of $10ms$ frame length.

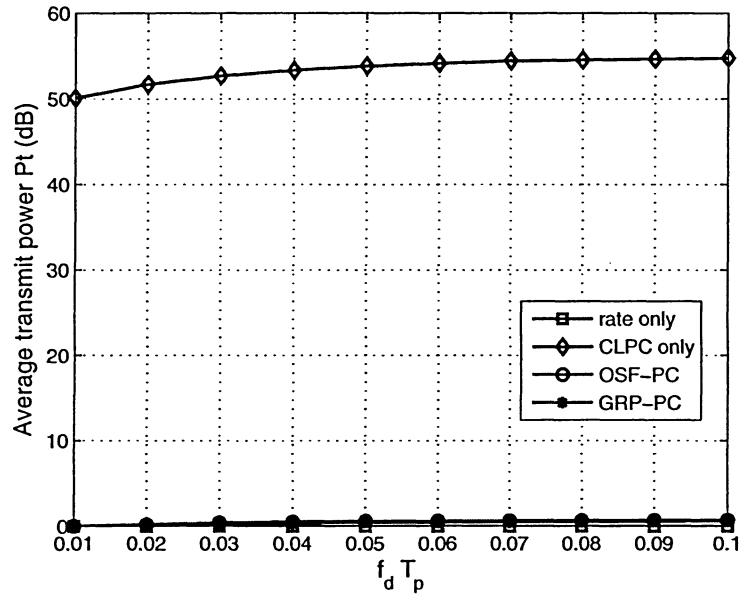

Figure 3.10: Average Transmit Power Consumption (a)

Next, we investigate the BER performance within these four methods with $10ms$ frame length shown in Fig. 3.13 and $2ms$ frame length shown in Fig. 3.14. BER is calculated based on using 3σ range of SIR distribution in these simulations. From the top to the bottom of both figures, the four curves represent rate adaptation, *OSF-PC*, *GRP-PC* and CLPC, respectively. The CLPC scheme achieves the best BER performance due to applying a fixed target CIR, while the tradeoff is the highest power consumption. Our proposed scheme

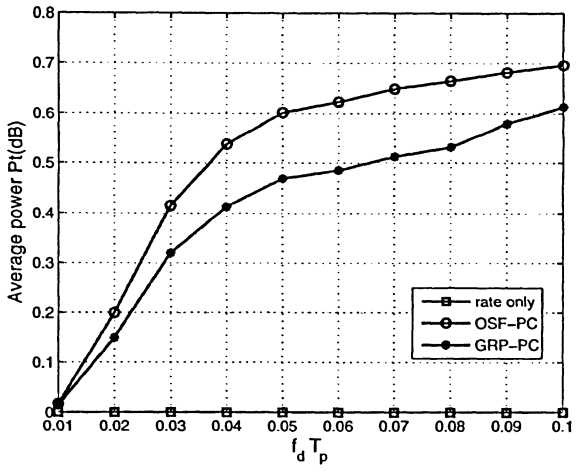

Figure 3.11: Average Transmit Power Consumption *vs.* f_dT_p with $10ms$ Frame Length

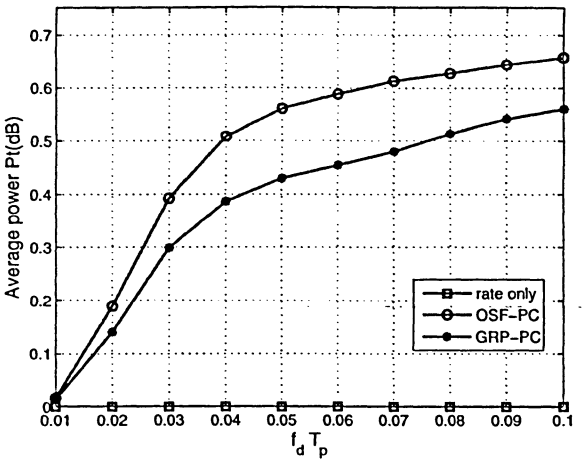

Figure 3.12: Average Transmit Power Consumption *vs.* f_dT_p with $2ms$ Frame Length

(*GRP-PC*) offers a better BER performance than that of the *OSF-PC* and rate adaptation scheme. It can also be explained that our proposed algorithm works more accurate than *OSF-PC* and rate adaptation scheme. It is observed that the case of shorter frame length ($2ms$) has a better BER performance than that of the $10ms$ frame length case. The reason is that the faster (shorter frame length) power control is capable of tracking the channel variation more precisely than longer frame length ($10ms$).

Finally, the performance of outage probability is examined. It is well known that the outage probability is an important parameter for the uplink. It is computed by calculating the fraction of the frames that a packet cannot be successfully transmitted because the received E_b/I_0 falls below a threshold (*i.e.*, 7dB) and needs to be retransmitted. From Fig. 3.15($10ms$ frame length) and Fig. 3.16($2ms$ frame length), it is obvious that the CLPC can achieve the lowest outage probability and our proposed algorithm (*GRP-PC*) again outperforms *OSF-PC* and rate adaptation schemes.

In this chapter, we proposed an algorithm of simultaneously adapting transmission power and data rate in an uplink UMTS WCDMA system. Greedy Rate Packing (GRP) is applied in the rate adaptation, which assigns the higher transmission rate to the users with

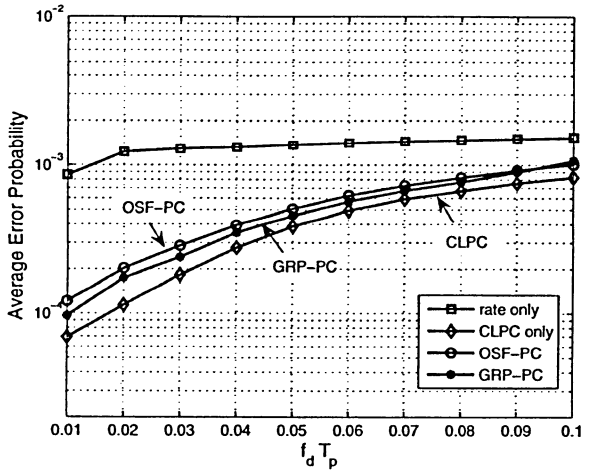

Figure 3.13: Average BER performance *vs.* $f_d T_p$ with $10ms$ Frame Length

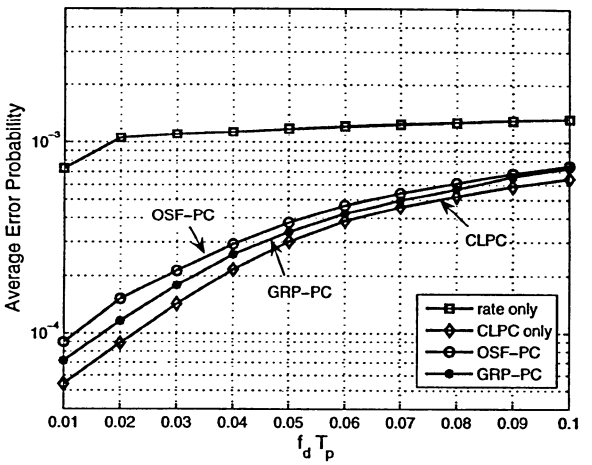

Figure 3.14: Average BER performance *vs.* $f_d T_p$ with $2ms$ Frame Length

better channel conditions meanwhile minimizing the transmission power. Consequently, the resource allocation works in an efficient way. Rate adaptation alone, CLPC alone, *OSF-PC* [75], and our proposed algorithm (*GRP-PC*) are evaluated and compared by the computer simulations. The numerical results show that our proposed algorithm (*GRP-PC*) can give satisfying performance when compared with the other three schemes.

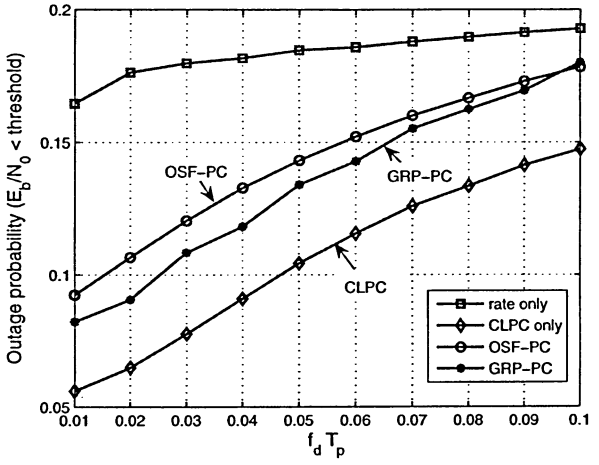

Figure 3.15: The Outage Probability *vs.* $f_d T_p$ with $10ms$ Frame Length

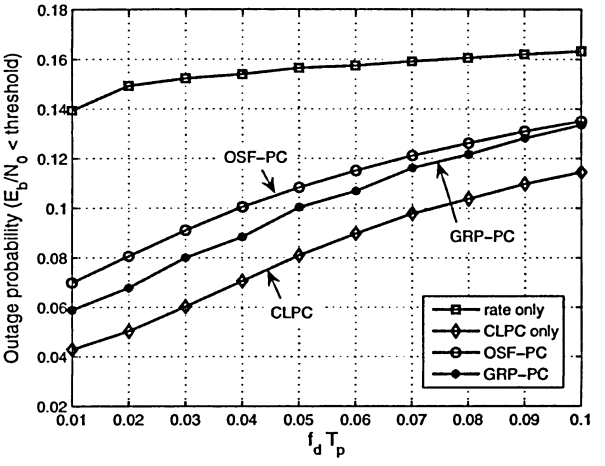

Figure 3.16: The Outage Probability *vs.* $f_d T_p$ with $2ms$ Frame Length

Chapter 4

Integrated Power Control and Rate Assignment with Variable Stepsize

Power control is an indispensable MAI combating and fading compensation technique in CDMA communications to track and compensate for the signal fluctuation. According to power update strategies, CLPC can be performed by using fixed stepsize power control (FSPC) algorithm and adaptive stepsize power control (ASPC) algorithm.

4.1 Problem Statement

The FSPC scheme is easy to operate and requires measurement of the received CIR. The measured value is compared to the desired target value. Depending on the comparison result, a power control command (PCC) of a "+1" or a "-1" is sent over a feedback channel by the BS and is executed at the MS to increase or decrease the transmission power level by a fixed stepsize (normally 1 dB). It has been shown in [59] that the optimal stepsize is a function of Doppler frequency. As a result, FSPC algorithm can not fully react to the changing of the fading fluctuations when mobile speed changes. With a typical ASPC algorithm [59], the current stepsize is related to the PCC history and the Doppler frequency. A well-designed ASPC algorithm can track fading variations and reduce CIR oscillations around the target CIR^*, *i.e.*, reduce the standard deviation of the received CIR.

In this section, we extend our combined power control and greedy rate packing (GRP) allocation scheme discussed in Section 3.3 by introducing a novel dynamic stepsize power

control (DSPC) algorithm [2]. It is known that the GRP algorithm maximizes the throughput by judiciously allocating the data rate to each user. With the GRP, there exists a set of discrete target $CIRs^*$, which create a multi-edge CIR region. The proposed variable stepsize scheme is based on the difference between the target CIR^* and the received CIR. During each power control cycle, the BS compares the received CIR with the target CIR^* to determine the current power control stepsize. If the region in which the received CIR falls is farther from the target CIR^*, a larger stepsize will be chosen to adjust the transmit power with a larger degree to well track the channel condition variation and to maintain the desired target value. Otherwise, a smaller stepsize will be used when the received CIR is closer to the target CIR^* to reduce the granular noise.

4.2 System Model

We consider a single cell W-CDMA system with N users. Suzuki process is defined as channel model and only uplink is concerned in this work. We applied the GRP to allocate the data rate, and correspondingly, the target CIR^*, of the users with the aid of their channel state information. While a dynamic stepsize power control (DSPC) algorithm is applied inside the frames to force the received CIR close to the target instead of fixed stepsize power control (FSPC) algorithm.

As mentioned before, the proposed DSPC scheme adjusts the power control stepsize by comparing the received CIR with the target CIR^*, and the stepsize is primarily dependent on the region in which the received CIR falls. The power update iteration algorithm at the $(t+1)$th time slot is given by

$$P_i(t+1)_{(dB)} = P_i(t)_{(dB)} + DS(t)_{(dB)} \tag{4.1}$$

$$DS(t)_{(dB)} = a_{(dB)} \cdot b \cdot z \tag{4.2}$$

where DS is a dynamic stepsize which is based on the initial stepsize a, dynamic component b, which is an integer, and z which is the conventional PCC, *i.e.*, "+1" or "-1", to determine

the transmission power to be either increased or to be decreased. The PCC is given by

$$z = \begin{cases} +1 & \xi_i < \xi_i^* \\ -1 & \xi_i > \xi_i^* \end{cases} \tag{4.3}$$

where ξ_i and ξ_i^* represent the received CIR and the target CIR^* of the ith user, respectively. Therefore, the absolute value of DS falls in the range $a \leq |DS| \leq DS_{max}$, where DS_{max} is a design parameter. The DSPC model is shown in Fig. 4.1. The MS transmitted signal power is updated with a variable stepsize every power control period. The output from the DS determination unit is transmitted to the MS via the downlink for transmit power control.

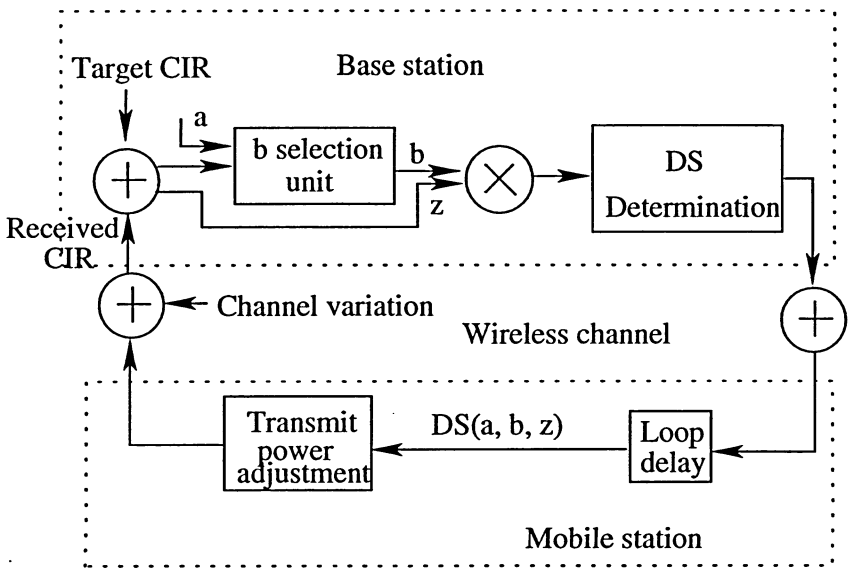

Figure 4.1: Dynamic stepsize Power Control Model

From Eq. (3.21), (3.22), (4.1) and (4.2), it is clear that the primary difference between the FSPC scheme and the proposed DSPC algorithm is a dynamic component b. Based on the power and rate allocation scheme proposed in Section 3.3, there exists a set of predefined nonzero discrete target CIR^*, $\Omega = \{\xi^{(1)*} < \xi^{(2)*} < \cdots < \xi^{(k)*}\}$ for each active user. Then, at the beginning of every frame, a target CIR^*, for example, the jth element from Ω, $\xi^{(j)*}$ as shown in Fig.4.2, is assigned to the active MS using the GRP algorithm presented in Section 3.3.2. The value of b can be chosen at the BS by comparing the received CIR with the target CIR^*. Fig. 4.2 shows an example of b selection scheme within multi-edge target

$CIRs^*$ region and the target CIR^* for the current frame is $\xi^{(j)*}$. If the region in which the received CIR falls is farther from the target CIR^*, then a larger b will be selected resulting in a larger stepsize to track the larger CIR deviation from the target. Otherwise, a smaller b will be used resulting in a smaller stepsize when the received CIR is closer to $\xi^{(j)*}$, leading to a smaller granular noise. From the example, we can see that the received CIR falls in the region between $\xi^{(j+1)*}$ and $\xi^{(j+2)*}$. As a result, b can be designated as 2. Besides, it should be noted that b is constrained by : $1 \leq b \leq DS_{max}/a$.

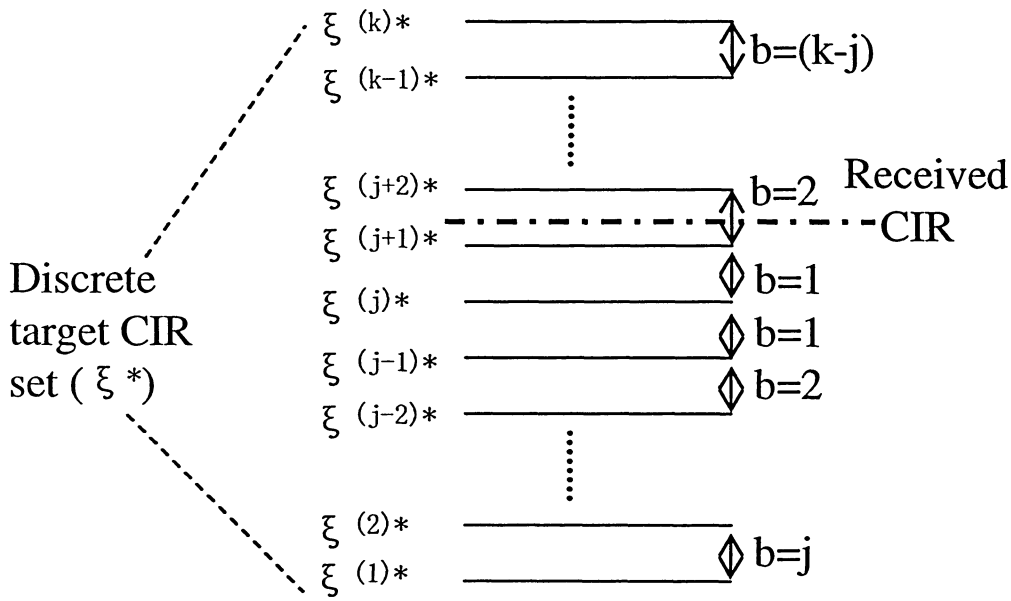

Figure 4.2: Dynamic Component b Selection Scheme within Multi-Edge CIR Region. The target CIR^* for the current frame is $\xi^{(j)*}$

4.3 Dynamic Stepsize Power Control Algorithm

The algorithm based on a frame/time slot structure for the selection of the dynamic component b and the transmission power adjustment is presented as follows.

Base station:

I. CIR target assignment: At the beginning of every frame, each user can be assigned a

target CIR^* by BS based on the channel conditions from the predefined discrete CIR target set Ω. Those inactive users wait for the next adaption cycle. Repeat following procedures for each active users.

II. Variable stepsize adjustment procedure: For a generic active user, assuming that the target CIR^* assigned is the jth element from Ω. At the beginning of every power control cycle T_p (time slot), set $b = 1$. By comparing the received CIR with the target $\xi^{(j)*}$, the following steps would be executed as follows:

(i) Received $CIR \geq \xi^{(j)*}$

Begin

z= -1;

FOR l= 1: $(k-j)$

IF Received $CIR \leq \xi^{(j+l)*}$ **THEN**

$DS = a \cdot b \cdot t$; exit from the FOR loop.

ELSE

b= b+1; $DS = a \cdot b \cdot t$;

IF$DS \geq DS_{max}$ **THEN**

DS= DS_{max}; exit from the FOR loop.

ENDIF

ENDIF

ENDFOR

End

(ii) Received $CIR < \xi^{(j)*}$

Begin

z= +1;

FOR l= 1: j

IF Received $CIR \geq \xi^{(j-l)*}$ **THEN**

$DS = a \cdot b \cdot t$; exit from the FOR loop.

ELSE

b= b+1; $DS = a \cdot b \cdot t$;

IF $DS \geq DS_{max}$ **THEN**

DS= DS_{max}; exit from the FOR loop.

ENDIF

ENDIF

ENDFOR

End

Mobile station:

I. Transmitted power adjustment: The MS adjusts the transmitted power by using the obtained DS in Eq. (4.1) and (4.2) in the range $P_{min} \leq P_i \leq P_{max}$.

4.4 Numerical results and discussions

In this section, we evaluate the performance of the proposed dynamic stepsize power control algorithm (DSPC) by comparing the results of applying fixed stepsize CLPC in the algorithm presented in Chapter 3, Section 3.3 (called FSPC algorithm). A frame/time slot structure of UMTS W-CDMA standard is employed in our simulation as shown in Fig. 1.4. The power control frequency is 1500Hz ($T_p = 1/1500s$). The chip rate and $(E_b/I_0)_{target}$ are assigned to be $5Mchips/s$ and 7 dB, respectively. In addition, the mobile user speed is set from 8.1 km/h to 81 km/h. Accordingly, the normalized Doppler frequency, f_dT_p, is in the range of 0.01 to 0.1. The initial stepsize, a, is set to be 0.5 dB and the maximum dynamic stepsize, DS_{max}, equals 2 dB in our simulations. Other physical layer parameters can be referred from Table 3.1 in Chapter 3, Section 3.3.3. The 2 ms frame length is also used in our simulations. In addition, some key parameters of power control , such as loop delay D, PCC transmission error, are examined as well.

Fig. 4.3 and Fig. 4.4 compare the throughput performance vs. the normalized Doppler frequency for the proposed DSPC algorithm and the FSPC algorithm corresponding to the case of 10 ms frame length and 2 ms, respectively. It is shown that the DSPC scheme offers higher average throughput than that of the FSPC scheme. The average throughput gain achieved is about 2% in the case of 10 ms frame length and 3.5% in the case of 2 ms frame length across the interested range. Furthermore, it is shown that system throughput is enhanced by using a shorter frame length ($2ms$).

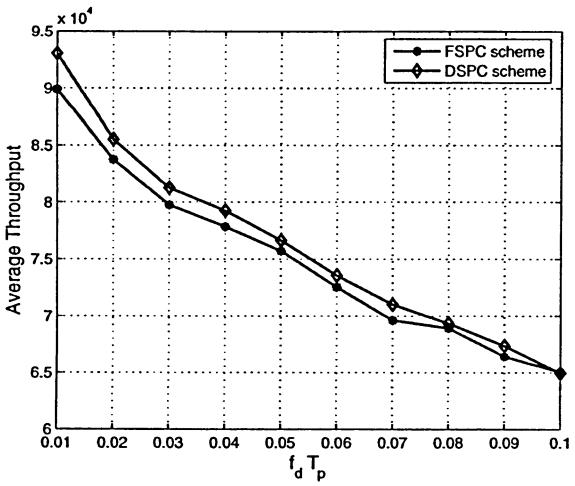

Figure 4.3: Average throughput for FSPC and DSPC Schemes with $10ms$ Frame Length

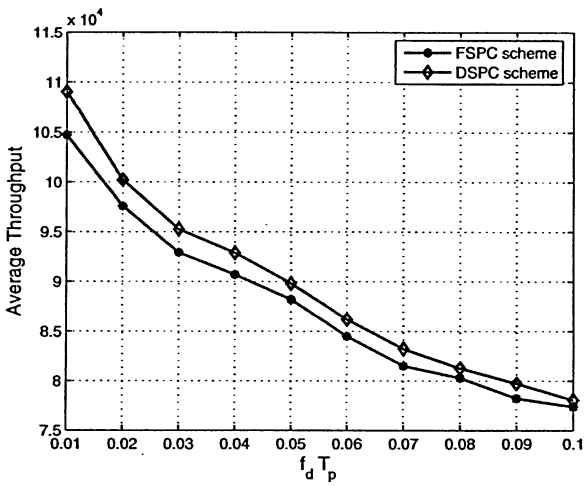

Figure 4.4: Average throughput for FSPC and DSPC Schemes with $2ms$ Frame Length

A comparison of the power consumption between DSPC and FSPC algorithms is presented in Fig. 4.5 with 10 ms frame length. It is observed that the average transmission power of the DSPC algorithm is lower than that of the FSPC algorithm with about 6.5% average power consumption saving. The reason can be explained that the FSPC scheme only uses fixed stepsize for power adjustment, while the proposed DSPC scheme dynamically adjusts the stepsize based on the difference between the received CIR and the target CIR^*. Thus the relative gain of power consumption is obtained by employing the DSPC scheme. Besides, a 2 ms frame length is applied in the simulation as well displayed in Fig.

4.6. It shows the same trend as the case of 10 ms frame length, where the DSPC algorithm consumes less power than FSPC scheme. Moreover, the less power consumption can be obtained by applying the shorter frame length (2 ms).

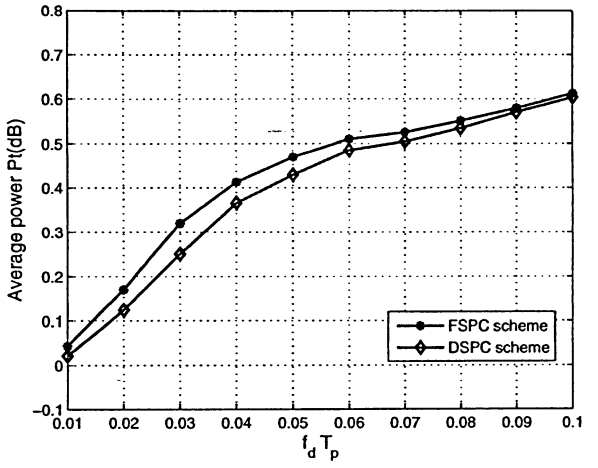

Figure 4.5: Average transmission power Consumption for FSPC and DSPC Schemes with 10ms Frame Length

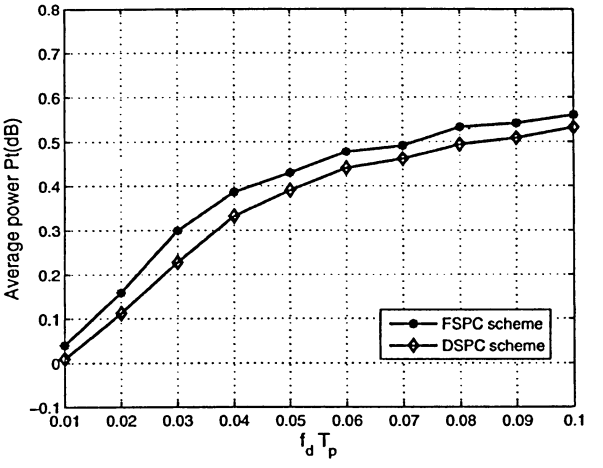

Figure 4.6: Average transmission power Consumption for FSPC and DSPC Schemes with 2ms Frame Length

System performance in terms of the BER and outage probability is evaluated in Fig. 4.7, Fig. 4.9 with 10 ms frame length and Fig. 4.8, Fig. 4.10 with 2 ms frame length, respectively. Again, the DSPC method has a better BER and lower outage probability than that of the FSPC method. It can be explained that the DSPC scheme works more accurate than the FSPC scheme. Besides, it should be noted that the BER and outage probability of DSPC algorithm are slightly better than that of the FSPC algorithm in the 10 ms frame length simulation. While DSPC algorithm applied in a shorter frame length structure (2 ms) can achieve considerably better BER and outage probability performance than FSPC algorithm. The reason for this is that our proposed algorithm uses variable stepsize which can track the target CIR^* and channel variations more accurately than the fixed stepsize algorithm, especially employing a shorter frame length.

Fig. 4.11 and Fig. 4.12 investigate the standard deviation (STD) of the received CIR at

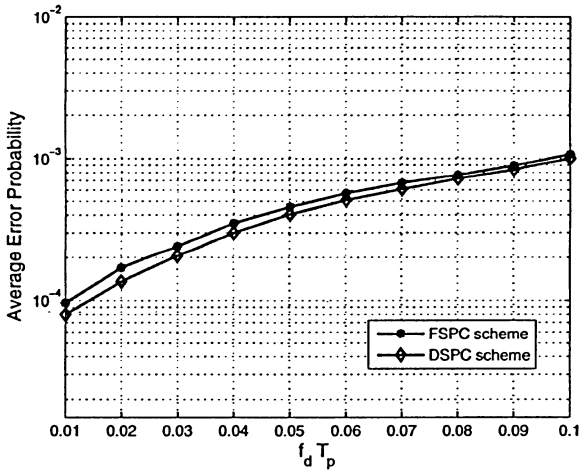

Figure 4.7: Performance of BER for FSPC and DSPC Schemes with $10ms$ Frame Length

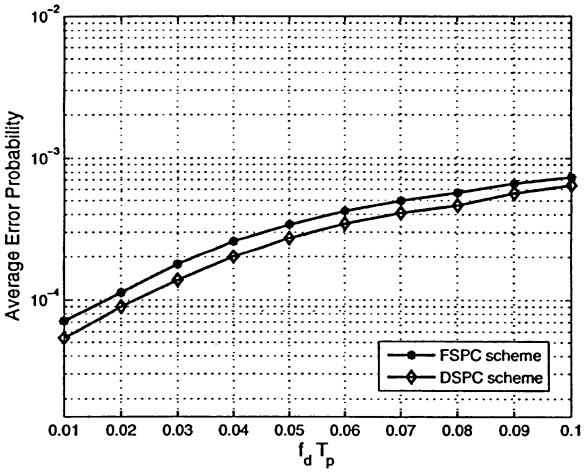

Figure 4.8: Performance of BER for FSPC and DSPC Schemes with $2ms$ Frame Length

the BS. It is noted that the STD of the received CIR monotonically increases with $f_d T_p$. It implies that it is harder to track the signal fluctuation due to fading when Doppler frequency increases. By using the proposed DSPC, there is a significant improvement of the tracking ability of the DSPC over FSPC. The gain of 0.5 dB (see Fig. 4.11) and 0.65 dB (see Fig. 4.12) can be observed in the interested range corresponding to 10 ms frame length and 2 ms frame length, respectively. In addition, we also examined the effect of different initial stepsize, a, employed in the DSPC, with 0.25 dB and 0.5 dB being compared. In lower mobile speed, the difference is not significant. When mobile speed increases, the larger value of a (0.5 dB) achieves better performance than that of the smaller value of a (0.25 dB). This can be explained that the channel variation is too large to be tracked with this small initial stepsize. Therefore, a= 0.5 dB is recommended for the proposed DSPC scheme.

Next, we move closer to real implementation of the power control algorithms and take into account some practical issues of imperfect power control in which power updating is subjective to feedback delay (PCC feedback delay) and PCC is subject to transmission error.

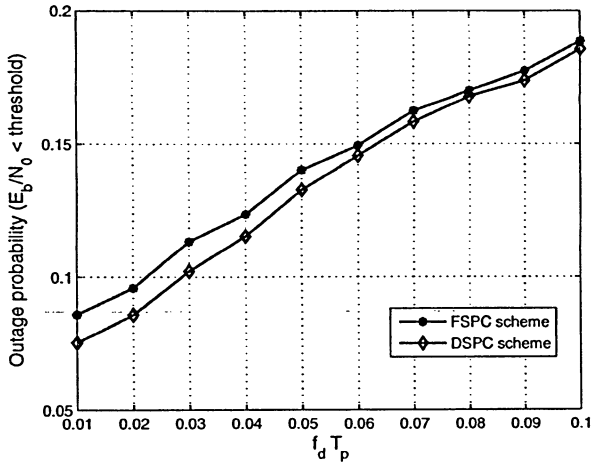

Figure 4.9: Performance of Outage Probability for FSPC and DSPC Schemes with $10ms$ Frame Length

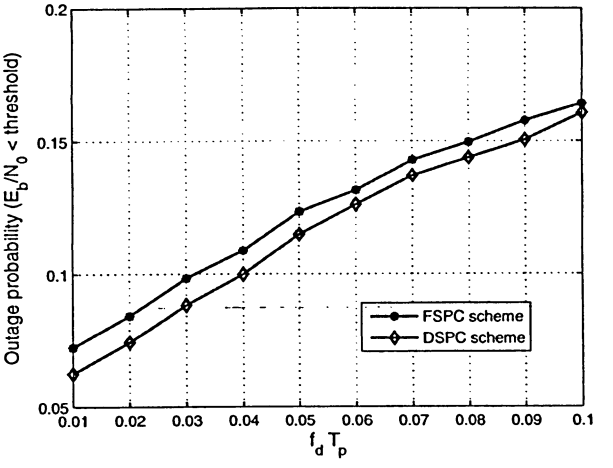

Figure 4.10: Performance of Outage Probability for FSPC and DSPC Schemes with $2ms$ Frame Length

As discussed in Chapter 3, Section 3.1.3, the feedback delay greatly affects the performance of a power control algorithm. [24] and [61] have shown that the effect of parameters' imperfections on the performance degradation is more significant on the variable stepsize algorithm than that on the fixed stepsize algorithm. The effect of loop delay is examined in Fig. 4.13 for FSPC algorithm and in Fig. 4.14 for DSPC algorithm, respectively. From the results shown in both figures, it can be observed that the BER performance degrades as feedback delay increases. Furthermore, the effect of feedback delay is more sensitive in DSPC algorithm than in FSPC scheme. We can see from Fig. 4.14 that with feedback delay of D=$2T_p$ and D=$3T_p$ the performance of DSPC algorithm is even worse than that of the FSPC algorithm, This is due to the lager error of power adjustments in the DSPC algorithm when the PCC bits are subject to the feedback delay.

The effect of PCC channel error rate is investigated with the case of $P_e = 10^{-1}$, $P_e = 10^{-2}$, and $P_e = 10^{-3}$. Fig. 4.15 and Fig. 4.16 exhibit the STD of received CIR vs. the normalized Doppler frequency for the proposed FSPC algorithm and the DSPC algorithm, respectively. Compare these two results, it is shown that the performance of DSPC degrades

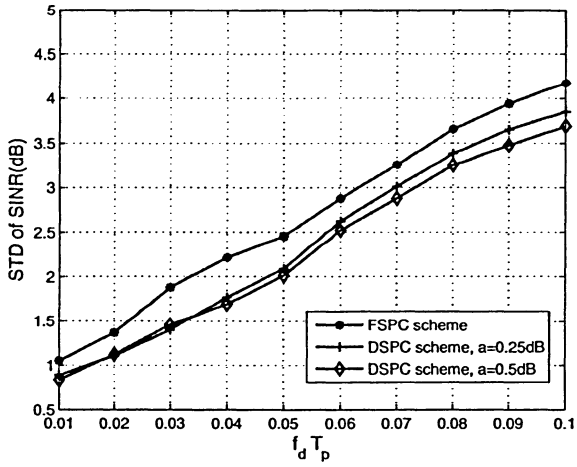

Figure 4.11: Standard Deviation of the Received CIR for FSPC and DSPC Schemes with $10ms$ Frame Length

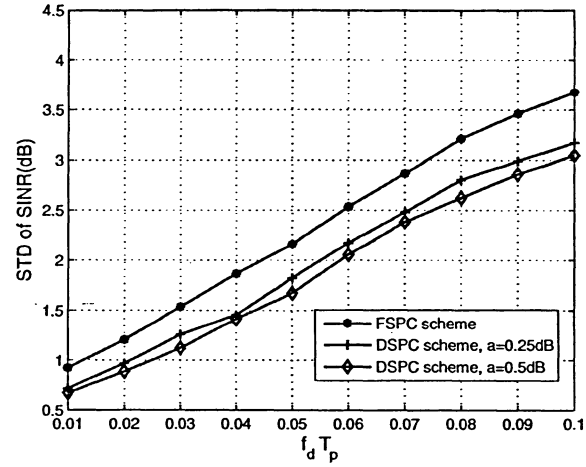

Figure 4.12: Standard Deviation of the Received CIR for FSPC and DSPC Schemes with $2ms$ Frame Length

more significantly and performance becomes worse than that of the FSPC when P_e increases, especially in the case of $P_e = 10^{-1}$. It is also observed that when the PCC channel error rate increases from 10^{-2} to 10^{-1}, the STD of the received CIR increases in the range of 2.75 dB for DSPC algorithm and 1.5 dB for FSPC algorithm. However, the STD of the received CIR only increases 0.5 dB for DSPC scheme and 0.35 dB for FSPC scheme when PCC channel error rate increase from 10^{-3} to 10^{-2}. These results suggest that the PCC channel error rate should be controlled to below 10^{-2} to optimize the power control performance.

In this chapter, we proposed a novel dynamic stepsize power control (DSPC) algorithm. The variable stepsize is determined by the difference between the target CIR^* and the received CIR. If the region in which the received CIR falls is farther from the target CIR^*, a larger stepsize is chosen to increase the tracking ability of the power control algorithm. Otherwise, a smaller stepsize is used when the received CIR is closer to the target CIR^* to reduce the granular noise. Simulation results demonstrated the effectiveness of the proposed DSPC algorithm when compared with the fixed stepsize power control (FSPC) scheme. It is expected that further improvement can be achieved by fine tune the design parameters.

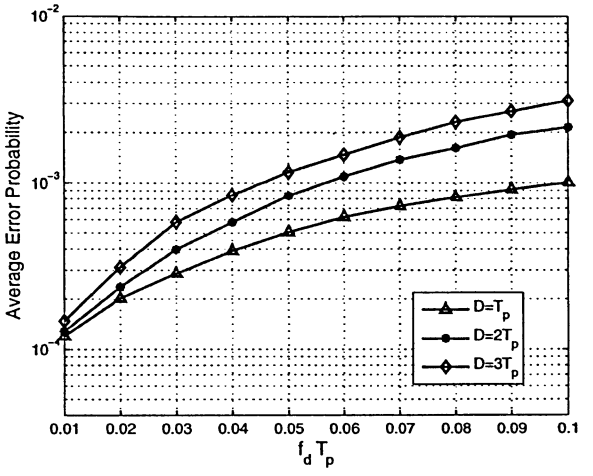

Figure 4.13: Effect of Feedback Delay on the BER Performance of FSPC Algorithm

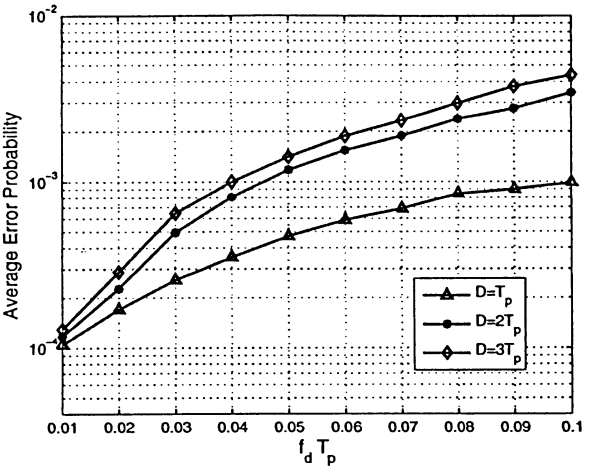

Figure 4.14: Effect of Feedback Delay on the BER Performance of DSPC Algorithm

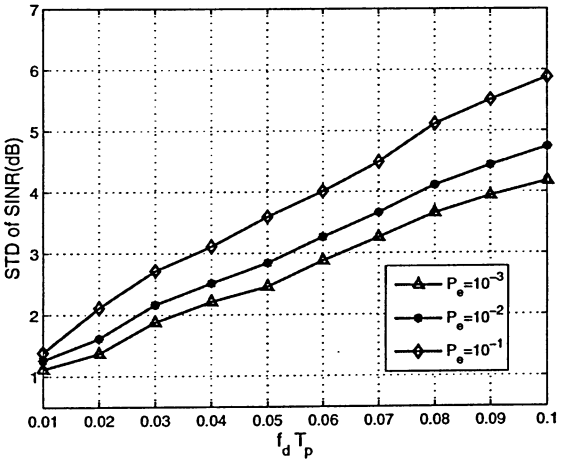

Figure 4.15: Effect of *PCC* Channel Error on STD of Received CIR for FSPC algorithm

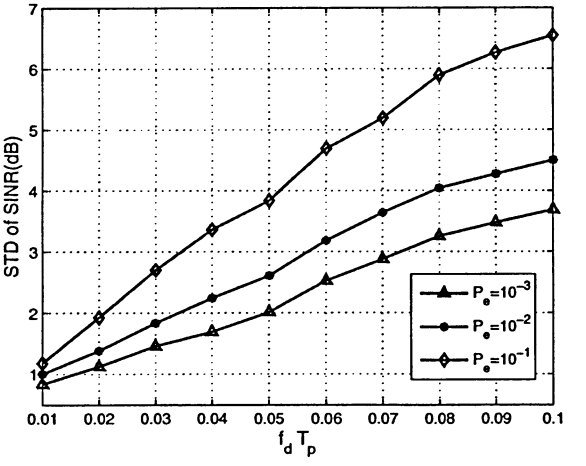

Figure 4.16: Effect of *PCC* Channel Error on STD of Received CIR for DSPC algorithm

Chapter 5

Conclusions and Future Work

Radio resource management plays an important role in the design of cellular radio systems. To allocate resources in real time for maximizing system capacity is an important task. Power control is one essential issue in this problem, in particular for CDMA systems. The 3G W-CDMA systems provide services characterized by being delay insensitive and offering a higher transmission rate while compared to the cellular system currently deployed, such as GSM, DS-CDMA. Appropriate network control for delay insensitive and multirate applications is straightforward to specify in next generation wireless networks. In this thesis, the main focus has been on heterogeneous resource allocation. The main objective has been to suggest power control based RRM methods, combined with adaptive rate transmission scheme.

5.1 Summary

We performed extensive background literature and patent search regarding the present state of the power control and adaptive rate transmission techniques in mobile cellular communication systems. Based on our literature review, we defined an enhancement to the existing power and rate control technique for UMTS W-CDMA systems. Two different subjects have been studied in this thesis. The first subject is the combined power control and rate assignment algorithm, and the second is a dynamic stepsize power control scheme.

We apply a heuristic greedy rate packing (GRP) algorithm to allocate the high data rate to channels with good quality. GRP has linear complexity and is executed in a cell-wise

manner. For a single cell and uplink direction, we found that the GRP scheme finds the optimal solution, which motivates its use under more general conditions too. It also constitutes a practical interpretation of the information theoretic water filling concept. Inevitably, this creates some unfairness among the users, so practically some mobility will be necessary if the resulting solution should also be fair in the long run. Fairness versus maximum throughput was not specifically part of the problem definition for this best effort service. It is known that GRP uses knowledge of link gains and assigns the rates within the cell, *i.e.*, slightly more information than a fully distributed scheme. This model is realistic when the resource allocation is done at each station but distributed between them. In principle, the transmission schemes applied for throughput maximization, allocate more rate and sometimes more power to good channels. That is, quite a different behavior from the usual SIR-based power control, which has its cause in the new application.

Our proposed combined power control and rate assignment algorithm starts with the process of target $CIR^{\star}$ assignment with the aid of users' channel information. Based on Eq. (3.14), the rate assignment and target $CIR^{\star}$ assignment are interchangeable. Thus, the user with good channel condition (higher channel gain) will be assigned higher data rate. Power control serves as an integrated role in CDMA systems: *power allocation* and *closed loop power control* (CLPC). Power allocation is an important resource management function for multiclass systems and is used to specify the target received power levels to satisfy the QoS requirement and peak power restrictions of all the users in the system. With a certain target $CIR^{\star}$ ($\xi_i^{\star}$) assignment, we allocate the transmission power in terms of Eq (3.20) to every user in the system. Then closed loop power control procedure starts to keep the CIR at the receivers at their target values. A detailed overview of power control in CDMA cellular systems has been given in the thesis.

Since in CDMA all users share simultaneously the same frequency band, they all interfere with one another. Therefore, the minimization of transmission powers leads to an increase in capacity. The fixed stepsize power control (FSPC) algorithm can not fully react to the changing of the fading fluctuations when mobile speed changes. The driving idea of the

proposed dynamic stepsize power control (DSPC)algorithm is the minimization of the received power level variance. The variance minimization leads to a reduction of transmission power consumption. With the GRP, there exists a set of discrete target CIR^*, which create a multi-edge CIR region. The proposed variable stepsize scheme is based on the difference between the target CIR^* and the received CIR. During each power control cycle, the BS compares the received CIR with the target $CIRs^*$ to determine the current power control stepsize. If the region in which the received CIR falls is farther from the target CIR^*, a larger stepsize will be chosen to adjust the transmit power with a larger degree to well track the channel condition variation and to maintain the desired target value. Otherwise, a smaller stepsize will be used when the received CIR is closer to the target CIR^* to reduce the granular noise.

Furthermore, we extend out proposed algorithms to a frame/time slot structure of the variable spreading gain W-CDMA system, where the transmission power is updated every time slot while the rate adaptation is employed frame by frame. The Suzuki process is defined as our channel model in a multi-user environment.

The performance of the proposed algorithms have been investigated through extensive computer simulation. The reference algorithms are Zhao *et al.* [75] (*OSF-PC*),the CLPC and rate adaptation alone schemes, in which the FSPC alogorithm is applied inside the frames to force the received CIR close to the target. The simulations indicate that significant improvements can be achieved with our proposed algorithms in comparison to the reference algorithms.

5.2 Open Problems

Clearly our proposed power control and adaptive date transmission algorithms can improve the system performance based on some ideal assumptions. Some interesting extensions of the algorithms proposed in this thesis can be continued to study as followed:

- *Channel prediction and CIR estimation errors.*

Due to the fact that we have assumed a perfect channel prediction and received CIR estimation in the simulations of our proposed algorithms, a possible future research contribution could be concerned about the prediction and estimation error. It is known that the estimation errors can be made smaller by increasing the average time of the measurement, but this might lead to a longer loop delay, which is undesirable. Besides, a more accurate long-range channel power prediction would lead to a more accurate channel power pdf, which could be more beneficial in our proposed techniques.

- *Feedback information accuracy*:

  The information of the CIR at the receiver should somehow be communicated to the transmitter. An accurate representation of the CIR measurement requires several bits, but this requires more signal overhead. This form of feedback is referred to as information feedback. In our proposed algorithms, we assumed that the feedback information was well sent back from BS to MS. The simulation results in Chapter 4, Section 4.4 suggest that the feedback channel error rate should be controlled to below 10^{-2} to optimize the power control performance. Thus, we may address the feedback inaccuracy issue, which will make the algorithm more close to the real application.

- *Fairness issue*:

  As mentioned already, the GRP algorithm maximizes the throughput by judiciously allocating the data rate to each user with the aid of their channel state information. If the users in a very bad channel condition (deep fade), they may be not assign any data rate. It leads to a fairness problem in a long run. Thus, a more conservative rate allocation scheme could deal with issues of a minimum required data rate combined with some rate scheduling strategies.

- *Power oscillation problem*

  In a wireless communications system, frequent variations occur in the radio interface. The received CIR may change dramatically and very fast. Either the FSPC or our

proposed DSPC algorithms, the transmission power will be adjusted and change even if the received CIR is very close to the target CIR^*. It leads to the power oscillation problem. One solution presented in [79] is to use an CIR margin M and define $CIR_{target} + M$ as the new power control target. Thus, it exists a stabilization zone, where the transmission power is kept stable. Based on this idea, we may modify our DSPC algorithm as follows:

IF $(1-\alpha)\cdot\xi^{(j)*} \leq \xi_{Received} \leq (1+\alpha)\cdot\xi^{(j)*}$ **THEN**
there is no power adjustment required, *i.e.*, $DS = 0$.

It implies that the algorithm can be improved based on tuning the parameter α.

- *Joint resource allocation and adaptive antennas*:

  Joint resource allocation and adaptive antennas is also an interesting topic. The results in [80] proposed scheduling combining with a rather different beamforming technique, aiming to increase the channel variance.

Bibliography

[1] G. Luo and L. Zhao, "Dynamic rate assignment and power control in uplink UMTS W-CDMA systems," *in Proc. IEEE Canadian Conference on Electrical and Computer Engineering (CCECE)*, May 2006.

[2] G. Luo and L. Zhao, "A novel dynamic stepsize power control algorithm for UMTS W-CDMA systems," *to appear in Proc. IEEE 6th International Conference on ITS Telecommunications (ITST)*, June 2006.

[3] E. Dahlman, B. Gudmundson, M. Nilsson, and J. Sköld, "UMTS/IMT-2000 based on Wideband CDMA," *IEEE Communications Magazine*, vol. 36, no. 9, pp. 70–80, 1998.

[4] "Universal Mobile Telecommunicaion System (UMTS) selection procedures for the choice of radio transmission technologies of the UMTS," *3GPP, ETSI TR 101 112 version 3.2.0*, 1998.

[5] E. Dahlman, P. Beming, J. Knutsson, F. Ovesjö, M. Persson, and C. Roobol, "WCDMA-The radio interface for future mobile multimedia communications,," *IEEE Trans. Vehicular Tech.*, vol. 47, no. 4, pp. 1105–1118, Nov. 1998.

[6] A. Fukasawa, T. Sato, Y. Takizawa, T. Kato, M. Kawabe, and R. E. Fisher, "Wideband CDMA system for personal radio communications," *IEEE Communications Magazine*, vol. 34, no. 10, pp. 116–123, Oct. 1996.

[7] M. Mousafa, I. Habib, and M. N. Naghshineh, "Efficient radio resource control in wireless networks," *IEEE Trans. Wireless Communications*, vol. 3, no. 6, pp. 2385–2395, Nov. 2004.

[8] D. M. Zhao, X. M. Shen, and J. W. Mark, "Radio resource management for cellular CDMA systems supporting heterogeneous service," *IEEE Trans. Mobile Computing*, vol. 2, no. 2, pp. 147–160, 2003.

[9] R. Vannithamby and E. S. Sousa, "Resource allocation and scheduling schemes for wcdma downlinks," *in Proc. IEEE Intl. Conf. Communications*, vol. 5, pp. 1406–1410, 2001.

[10] Z. Gajic, D. Skataric, and S. Koskie, "Optimal SIR-based power updates in wireless CDMA communication systems," *IEEE Conference on Decision and Control*, vol. 5, pp. 5146–5151, Dec. 2004.

[11] R. D. Yates, "A framework for uplink power control in cellular radio systems," *IEEE J. Select. Areas Communications*, vol. 13, no. 7, pp. 1341–1347, Sept. 1995.

[12] M. L. Sim, E. Guanawan, B. H. Soong, and C. B. Soh, "Performance study of close-loop power control algorithms for a cellular CDMA system," *IEEE Trans. Vehicular Tech.*, vol. 48, no. 3, pp. 911–921, May 1999.

[13] A. Chockalingam, P. Dietrich, L. B. Milstein, and R. R. Rao, "Performace of closed-loop power control in DS-CDMA cellular systems," *IEEE Trans. Vehicular Tech.*, vol. 47, no. 3, pp. 774–789, Aug. 1998.

[14] B. Hashem and E. S. Sousa, "On the capacity of cellular DS/CDMA systems under slow Rician/Rayleigh-fading channels," *IEEE Trans. Vehicular Tech.*, vol. 49, no. 5, pp. 1752–1759, Sept. 2000.

[15] L. Zhao and J. W. Mark, "Performance analysis of rate adaptation in WCDMA communication systems," *in Proc. IEEE Wireless Communications and Networking Conf.*, vol. 3, pp. 1400–1405, Mar. 2004.

[16] D. I. Kim, E. Hossain, and V. K. Bhargava, "Dynamic rate adaptation and integrated rate and error control in cellular WCDMA networks," *IEEE Trans. Wireless Communications*, vol. 3, no. 1, pp. 35–49, Jan. 2004.

[17] Y. K. Kwok and V. K. N. Lau, "System modeling and performance evaluation of rate allocation schemes for packet data service in wideband CDMA systems," *IEEE Trans. Computers*, vol. 52, no. 6, pp. 804–814, 2003.

[18] R. Mo, Y.H. Chew, and C. C. Chai, "Capacity of DS/CDMA system under multipath fading with different adaptive rate adaptive power schemes," *in Proc. IEEE Wireless Communications and Networking Conf.*, vol. 1, pp. 190–195, Mar. 2003.

[19] S. A. Jafar and A. Goldsmith, "Optimal rate and power adaptation for multirate CDMA," *in Proc. IEEE Vehicular Technology Conf.*, vol. 3, pp. 994–1000, Sept. 2000.

[20] K. K. Leung and L. C. Wang, "Integrated link adaptation and power control to improve error and throughput performance in broadband wireless packet networks," *IEEE Trans. Wireless Communications*, vol. 1, no. 4, pp. 610–629, Oct. 2002.

[21] B. Hashem and E. S. Sousa, "Reverse link capacity and interference statistics of a fixed-step power-controlled dc/cdma system under slow multipath fading," *IEEE Trans. Communications*, vol. 47, no. 12, pp. 1905–1912, Dec. 1999.

[22] A. Kurniawan, "Effect of feedback delay on fixed step and variable step power control algorithms in CDMA systems," *in Proc. IEEE Intl. Conf. Communications*, vol. 2, pp. 1096–1100, Nov. 2002.

[23] M. L. Sim, E. Gunawan, C. B. Soh, and B. H. Soong, "Characteristics of closed loop power control algorithms for a cellular DS/CDMA system," *IEEE Proc. Communications*, vol. 1145, no. 5, pp. 355–362, Oct. 1998.

[24] C. C. Lee and R. Steele, "Closed-loop power control in CDMA systems," *IEEE Proc. Communications*, vol. 143, no. 4, pp. 231–239, Aug. 1996.

[25] S. Ulukus and R. D. Yates, "Adaptive power control with MMSE multiuser detectors," *in Proc. IEEE Intl. Conf. Communications*, vol. 1, pp. 361–365, 1997.

[26] W. Li, C. L. Law, and V. K. Dubey, "A multistep power control algorithm for land mobile satellite with high dynamic channel," *in Proc. IEEE Vehicular Technology Conf.*, vol. 4, pp. 2965–2969, May 2001.

[27] F. Berggren and S. L. Kim, "Engergy-efficient control of rate and power in DS-CDMA systems," *IEEE Trans. Wireless Communications*, vol. 3, no. 3, pp. 725–733, May 2004.

[28] D. M. Novakovic and M. L. Dukic, "Evolution of the power control techniques for DS-CDMA toward 3G wireless communication systems," *IEEE Communications Surveys. http://www.comsoc.org/pubs/surveys*, Fourth Quarter 2000.

[29] W. C. Y. Lee, "Overview of cellular cdma," *IEEE Trans. Vehicular Tech.*, vol. 40, no. 2, pp. 291–302, May 1991.

[30] T. S. Rappaport, *Wireless Communications, Second Edition*, Pearson Education, Inc., 2002.

[31] J. G. Proakis, *Digital Communications, Fourth Edition*, McGraw-Hill, 2000.

[32] W. C. Y. Lee, *Mobile Communications Engineering, Second Edition*, McGraw-Hill, 1997.

[33] J. W. Mark and W. Zhuang, *Wireless Communications and Networking*, Perason Education, Inc., 2003.

[34] F. Adachi, M. Sawahashi, and K. Okawa, "Tree-structued generation of orthogonal spreading codes with different length for forward link of DS-CDMA mobile radio," *IEEE Electronic Letters*, vol. 33, no. 1, pp. 27–28, Jan. 1997.

[35] E. Dinan and B. Jabbari, "Spreading codes for direct sequence cdma and wideband cdma cellular networks," *IEEE Communications Magazine*, vol. 36, no. 9, pp. 48–54, Sept. 1998.

[36] B. Sklar, "Rayleigh fading channels in mobile digital communication systems part I: characterization," *IEEE Communications Magazine*, vol. 35, pp. 136–146, Sept. 1997.

[37] J. B. Anderson, T. S. Rappaport, and S. Yoshida, "Propagation measurements and models for wireless communications channels," *IEEE Communications Magazine*, vol. 33, no. 1, pp. 42–49, Jan. 1995.

[38] W. C. Jakes, *Microwave Mobile Communications*, New York, Wiley, 1993.

[39] H. Suzuki, "A statistical model for urban radio propogation," *IEEE Trans. Communications*, vol. 25, no. 7, pp. 673–680, 1977.

[40] M. Patzold, U. Killat, and F. Laue, "A deterministic digital simulation model for Suzuki processes with application to a shadowed Rayleigh land mobile radio channel," *IEEE Trans. Vehicular Tech.*, vol. 45, no. 2, pp. 318–331, May 1996.

[41] S. M. Alamouti, "A simple transmit diversity technique for wireless communications," *IEEE J. Select. Areas Communications*, vol. 16, no. 8, Oct. 1998.

[42] M. Moustafa, I. Habib, M. Naghshineh, and M. Guizani, "QoS-Enabled broadband mobile access to wireline network," *IEEE Communications Magazine*, vol. 40, pp. 50–56, Apr. 2002.

[43] J. T. Wu and E. Geraniotis, "Power control in multi-media CDMA networks," *in Proc. IEEE Vehicular Technology Conf.*, vol. 2, pp. 789–793, July 1995.

[44] J. W. Mark and S. Zhu, "Power control and rate allocation in multirate wideband CDMA systems," *in Proc. IEEE Wireless Communications and Networking Conf.*, vol. 1, pp. 168–172, Sept. 2000.

[45] L. Zhao, J. W. Mark, J. Ding, and W. C. Pye, "Power control and call admission in multirate wideband CDMA systems," *in Proc. IEEE Wireless Communications and Networking Conf.*, vol. 3, pp. 1583–1588, Mar. 2004.

[46] S. A. Grandhi, R. Vijayan, D. J. Goodman, and J. Zander, "Centralized power control in cellular radio system," *IEEE Trans. Communications*, vol. 42, no. 2, pp. 226–228, Feb. 1994.

[47] Q. Wu, W. Wu, and J. Zhou, "Centralized power control in CDMA cellular mobile systems," *IEEE Trans. Vehicular Tech.*, vol. 2, pp. 1268–1271, May 1997.

[48] M. Elmustrati and H. Koivo, "Centralized algorithm for the tradeoff between total throughput maximization and total power minimization in cellular systems," *IEEE Trans. Vehicular Tech.*, vol. 3, pp. 1598–1602, Oct. 2003.

[49] S. A. Grandhi, R. Vijayan, and D. J. Goodman, "Distributed cochannel interference control in cellular radio systems," *IEEE Trans. Vehicular Tech.*, vol. 42, no. 4, pp. 466–468, Nov. 1993.

[50] L. Lv, S. Zhu, and S. Dong, "Fast convergence distributed power control algorithm for WCDMA systems," *IEEE Proc. Communications*, vol. 150, pp. 134–140, Apr. 2003.

[51] D. Kim, K. Chang, and S. Kim, "Efficient distributed power control for cellular mobile systems," *IEEE Trans. Vehicular Tech.*, vol. 46, no. 2, pp. 313–319, May 1997.

[52] S. Ariyavistiakul and L. F. Chang, "Signal and interference statistics of a CDMA system with feedback power control," *IEEE Trans. Communications*, vol. 41, pp. 1626–1634, Nov. 1993.

[53] W. W. Tam and C. M. Lau, "Analysis of power control and its imperfections in CDMA cellular systems," *IEEE Trans. Vehicular Tech.*, vol. 48, no. 5, pp. 1706–1717, Sept. 1999.

[54] S. Ariyavisitakul, "Signal and interference statistics of a CDMA system with feedback power control - part II," *IEEE Trans. Communications*, vol. 42, no. 2, pp. 597–605, Feb. 1994.

[55] Y. Yang and J. Chang, "A strength-and-SIR-combined adaptive power control for CDMA mobile radio channels," *IEEE Trans. Vehicular Tech.*, vol. 48, no. 6, pp. 1996–2004, Nov. 1999.

[56] A. Sampath, P. Kuma, and J. Holtzman, "On setting reverse link target SIR in a CDMA system," *in Proc. IEEE Vehicular Technology Conf.*, vol. 2, pp. 929–933, May 1997.

[57] C. Koo, S. Shin, R. A. Difazio, D. Grieco, and A. Zeira, "Outer loop power control using channel-adaptive processing for 3G WCDMA," *in Proc. IEEE Vehicular Technology Conf.*, vol. 1, pp. 490–494, Apr. 2003.

[58] C. W. Sung and W. S. Wong, "A distributed fixed-step power control algorithm with quantization and active link quality protection," *IEEE Trans. Vehicular Tech.*, vol. 48, no. 2, pp. 553–562, Mar. 1999.

[59] L. Zhao and J. W. Mark, "Multi-step closed-loop power control using linear receivers for DS-CDMA systems," *IEEE Trans. Wireless Communications*, vol. 3, no. 6, pp. 2141–2155, Nov. 2004.

[60] R. R. Gejji, "Forward-link-power control in CDMA cellular systems," *IEEE Trans. Vehicular Tech.*, vol. 41, no. 4, pp. 532–536, Nov. 1992.

[61] S. Ariyavisitakul, "SIR based power control in a CDMA system," *Proc. IEEE Globecomm Conf.*, vol. 2, pp. 868–873, Dec. 1992.

[62] S. Ariyavisitakul, "A unified approach to the performance analysis of digital communication over generalized fading channels," *Proc. of IEEE*, vol. 86, no. 9, Sept. 1998.

[63] D. A. Jafar and A. Goldsmith, "Adaptive multirate CDMA for uplink throughput maximization," *IEEE Trans. Wireless Communications*, vol. 2, no. 2, pp. 218–228, Mar. 2003.

[64] S. Oh, D. Zhang, and K. M. Wasserman, "Optimal resource allocation in multiservice CDMA networks," *IEEE Trans. Communications*, vol. 2, no. 4, pp. 811–821, July 2003.

[65] S. Kahn, M. K. Gurcan, and O. O. Oyefuga, "Downlink throughput optimization for wideband CDMA systems," *IEEE Communication Letters*, vol. 7, pp. 251–253, May 2003.

[66] S. J. Oh and K. M. Wasserman, "Dynamic spreading gain control in multiservice CDMA networks," *IEEE J. Select. Areas Communications*, vol. 17, no. 5, pp. 918–927, May 1999.

[67] C. Mihailescu, X. Lagrange, and P. Godlewski, "Radio resource management for packet transmission in UMTS WCDMA system," *in Proc. IEEE Vehicular Technology Conf.*, vol. 1, pp. 573–577, Sept. 1999.

[68] L. Tong and P. Ramanathan, "Adaptive power and rate allocation for service curve assurance in DS-CDMA network," *IEEE Trans. Wireless Communications*, vol. 3, no. 2, pp. 555–564, Mar. 2004.

[69] C. C. Chai, T. T. Tjhung, and L. C. Leck, "Combined power and rate adaptation for wireless cellular systems," *IEEE Trans. Wireless Communications*, vol. 4, no. 1, pp. 6–13, Jan. 2005.

[70] S. Kandukuri and S. Boyd, "Simultaneous rate and power control in multirate multimedia CDMA systems," *Proc. Intl. Symposium on Spread Spectrum Techniques and Applications*, pp. 570–574, June 2000.

[71] S. Ulukus and L. J. Greenstein, "Throughput maximization in CDMA uplinks using adaptive spreading and power control," *Proc. Intl. Symposium on Spread Spectrum Techniques and Applications*, vol. 2, pp. 565–569, 2000.

[72] C. Li, X. Wang, and D. Reynolds, "Utility-based joint power and rate allocation for downlink CDMA with blind multiuser detection," *IEEE Trans. Wireless Communications*, vol. 4, no. 3, pp. 1163–1174, May 2005.

[73] A. Subramanian and A. H. Sayed, "Joint rate and power control algorithms for wireless networks," *IEEE Trans. Signal Processing*, vol. 53, no. 11, pp. 4204–4214, Nov. 2005.

[74] M. S. Bahaei, M. M. Kinggue, and G. Charbit, "Joint optimisation of outer-loop power control and rate adaptation over fading channels," *in Proc. IEEE Vehicular Technology Conf.*, vol. 3, pp. 26–19, Sept. 2004.

[75] L. Zhao and J. W. Mark, "Integrated power control and rate allocation for radio resource management in uplink WCDMA systems," *Proc. IEEE International Symposium on a World of Wireless, Mobile and Multimedia Networks (WoWMoM)*, June 2005.

[76] A. Sampath, P. S. Kumar, and J. M. Holtzman, "Power control and resource management for a multimedia CDMA wireless system," *in Proc. IEEE Intl. Symposium on Personal, Indoor and Mobile Radio Communications*, vol. 1, pp. 21–25, May 1995.

[77] Z. Q. Wang, "Expert's Forum - wireless telecommunications and 3G technology prospects," *http://www.huawei.com/publications*, vol. 15, Nov. 2005.

[78] H. Shao, C. Shen, D. Gu, J. Zhang, and P. Orlik, "Dynamic resource control for high-speed downlink packet access wireless channel," *Proc. IEEE Distributed Computing Systems Workshops*, pp. 838–843, May 2003.

[79] J. Nasreddine, L. Nuaymi, and X. Lagrange, "Adaptive power control algorithm for 3G cellular CDMA networks," *in Proc. IEEE Vehicular Technology Conf.*, vol. 2, pp. 984–988, May 2004.

[80] P. Viswanath, D. N. C. Tse, and R. Laroia, "Opportunistic beamforming using dumb antennas," *IEEE Trans. Inform. Theory*, vol. 48, no. 6, pp. 1277–1294, June 2002.